A pH-sensitive and Voltage-dependent Proton Conductance in the Plasma Membrane of Macrophages

ANDRAS KAPUS,* ROBERT ROMANEK,* ANTHONY YI QU,* ORI D. ROTSTEIN,‡ and SERGIO GRINSTEIN*

From the *Division of Cell Biology, The Hospital for Sick Children, Toronto, Canada M5G 1X8; and ‡Department of Surgery, Toronto General Hospital, Toronto, Canada M5G 2C4

ABSTRACT Phagocytes generate large amounts of metabolic acid during activation. Therefore, the presence of a conductive pathway capable of H^+ extrusion has been suggested (Henderson, L. M., J. B. Chappell, and O. T. G. Jones. 1987. *Biochemical Journal.* 246:325–329.). In this report, electrophysiological and fluorimetric methods were used to probe the existence of a H^+ conductance in murine peritoneal macrophages. In suspended cells, recovery of the cytosolic pH (pH_i) from an acid-load in Na^+ and HCO_3^--free medium was detectable in depolarizing but not in hyperpolarizing media. The rate of alkalinization was potentiated by the rheogenic ionophore valinomycin. These findings are consistent with the existence of a conductive H^+ (equivalent) pathway. This notion was confirmed by patch-clamping and fluorescence ratio measurements of single adherent cells. When voltage was clamped in the whole-cell configuration, depolarizing pulses induced a sizable outward current which was accompanied by cytosolic alkalinization. Several lines of evidence indicate that H^+ (equivalents) carry this current: (*a*) the conductance was unaffected by substitution of the major ionic constituents of the intra- and/or extracellular media, (*b*) the reversal potential of the tail currents approached the H^+ equilibrium potential; and (*c*) the voltage-induced currents and pH_i changes were both Zn^{2+} sensitive and had similar time course and potential dependence. The peak whole-cell current displayed marked outward rectification and was exquisitely H^+ selective. At constant voltage, the H^+ permeability was increased by lowering pH_i but was inhibited by extracellular acidification. Together with the voltage dependence of the conductance, these features ensure that H^+ extrusion can occur during activation, while potentially deleterious acid uptake is precluded. The properties of the conductance appear ideally suited for pH_i regulation during phagocyte activation, because these cells undergo a sustained depolarization and an incipient acidification when stimulated. Comparison of the magnitude of the current with the amount of metabolic acid generated during macrophage activation indicates that the conductance is sufficiently large to contribute to the H^+ extrusion required for maintenance of pH_i.

Address correspondence to Sergio Grinstein, Division of Cell Biology, Hospital for Sick Children, 555 University Avenue, Toronto, M5G 1X8, Canada.

J. GEN. PHYSIOL. © The Rockefeller University Press · 0022-1295/93/10/0729/32 $2.00
Volume 102 October 1993 729–760

INTRODUCTION

Phagocytes are attracted to sites of infection where they eliminate invading organisms by a combination of microbicidal mechanisms which include phagocytosis, secretion of lytic enzymes, and production of toxic oxygen metabolites (Sha'afi and Molski, 1988). The latter are derived from the one-electron reduction of molecular oxygen, catalyzed by a membrane bound multisubunit oxidase. NADPH, the immediate source of redox energy for this reaction, is generated and replenished by the hexose monophosphate shunt (Rossi, 1986; Clark, 1990). Activation of these reactions during phagocyte stimulation is associated with a massive burst of intracellular H^+ (equivalent) generation. Despite this increase in the rate of metabolic acid production, however, the intracellular pH (pH_i) of stimulated phagocytes remains at or above neutrality, even in the nominal absence of bicarbonate (Molski, Naccache, Volpi, Wolpert, and Sha'afi, 1980; Grinstein and Furuya, 1986). Under these conditions, two systems capable of effective H^+ extrusion have been described in both neutrophils and macrophages: (*a*) the ubiquitous Na^+/H^+ antiport is activated directly by the incipient cytosolic acidification and also by a receptor-mediated effect of the chemoattractants (Simchowitz and Cragoe, 1987; Grinstein and Furuya, 1986); (*b*) in addition, a vacuolar-type H^+ pump was recently reported to contribute to the extrusion of metabolic acid from phagocytes (Swallow, Grinstein, and Rotstein 1988).

In some excitable tissues, a third mechanism capable of H^+ extrusion during cell stimulation has been proposed. A voltage-dependent H^+ conductance which is activated upon depolarization has been studied in detail in snail neurons (Thomas and Meech, 1982; Byerly, Meech, and Moody, 1984; Byerly and Suen, 1989). Because in neurons, the membrane potential (E_m) can become more positive than the H^+ equilibrium potential (E_{H^+}) during physiological depolarization, this conductive pathway could mediate net acid efflux from the cells, contributing to pH_i homeostasis. In this context, it is noteworthy that phagocytes are known to undergo a large and sustained depolarization during activation (see Gallin, 1991, for review). Thus, H^+ extrusion could potentially take place in these cells via a conductive pathway. In neutrophils, the existence of a H^+ conductance has in fact been inferred from indirect evidence. Henderson and colleagues (Henderson et al., 1987, 1988) have shown that in activated cells E_m is altered by varying the transmembrane pH gradient. These authors also showed that Zn^{2+} and Cd^{2+}, which block the H^+ channels of neurons (Byerly et al., 1984; Mahaut-Smith, 1989), accentuated the cytosolic acidification of activated neutrophils, ostensibly by preventing conductive H^+ efflux (Henderson et al., 1988). More recent experiments have shown that, under conditions where the protonmotive force is kept constant by minimizing the metabolic burst, an increased H^+ (equivalent) permeability can be demonstrated in stimulated human (Nanda and Grinstein, 1991*a*) and porcine (Kapus, Szaszi, and Ligeti, 1992) neutrophils. In addition, a H^+ selective conductance was recently detected in cultured HL60 cells differentiated along the granulocytic path (Demaurex, Grinstein, Jaconi, Schlegel, Lew, and Krause, 1993).

The objective of the present experiments was to determine whether elicited macrophages, isolated from the peritoneal cavity of mice, possess a H^+ conductive pathway which could participate in pH_i regulation by mediating metabolic acid

extrusion during depolarization. Macroscopic fluorescence determinations of cell suspensions, single-cell fluorescence ratio determinations and patch clamping in the whole-cell configuration were used for this purpose.

MATERIALS AND METHODS

Materials

Powdered Brewer's thioglycolate was purchased from Difco Laboratories, Inc. (Detroit, MI). Calcium- and magnesium-free Hanks' balanced salt solution was obtained from Gibco Laboratories (Grand Island, NY).

2-[*N*-morpholino]ethanesulfonic acid (MES), *N*-[2-hydroxyethyl]piperazine-*N'*-[ethanesulfonic acid] (HEPES), piperazine-*N,N'*-bis[2-ethanesulfonic acid] (Pipes), valinomycin and medium RPMI-1640 (bicarbonate-free) were obtained from Sigma Chemical Co. (St. Louis, MO), and tris[hydroxymethyl]aminomethane (Tris) from Boehringer-Mannheim Corp. (Indianapolis, IN). *N*-methyl-D-glucamine was from Aldrich Chemical Co. (Milwaukee, WI). Both the free acid and the acetoxymethyl ester forms of 2',7'-bis-(2-carboxyethyl)-5(and 6)carboxyfluorescein (BCECF) were purchased from Molecular Probes Inc. (Eugene, OR). Bafilomycin A_1 was a kind gift from Professor K. Altendorf (Universität Osnabruck, Germany). All other reagents were of analytical grade and obtained from Sigma Chemical Co., Aldrich Chemical Co., Fisher Scientific (Pittsburgh, PA), or BDH Inc. (Toronto, Canada).

Solutions

The K^+ medium used during the macroscopic (population) fluorescence studies contained 140 mM KCl, 1 mM $CaCl_2$, 1 mM $MgCl_2$, 10 mM glucose and 20 mM HEPES-K (pH 7.4). The *N*-methyl-D-glucammonium$^+$ (NMG) medium was made by isosmotic replacement of 135 mM KCl, in the previous formulation, with the chloride salt of NMG and titration of HEPES with *N*-methyl-D-glucamine. The osmolarity of these media was adjusted to 295 ± 5 mosM with the major salt.

The composition of the buffers used for the patch clamp/single-cell fluorescence experiments is shown in Table I. All of these solutions also contained 1 mM $MgCl_2$ and 1mM ethylene glycol-bis (β-amino-ethyl ether)*N,N,N',N'*-tetraacetic acid (EGTA), except in the case when Zn^{2+} was used. For the latter experiments EGTA was omitted and $ZnCl_2$ was added to a final concentration of 0.2 or 2 mM, as indicated. Note that even in the aspartate-rich solutions, a low concentration of chloride was present to avoid electrode polarization. When one of the above solutions was used to fill the patch pipette, MgATP was added to a final concentration of 1 mM. Also, 300 μM BCECF (free acid) was added to the pipette when cells were preloaded with the acetoxymethyl ester of the dye for simultaneous fluorescence and electrophysiological determinations.

Cell Isolation and Characterization

Peritoneal macrophages were obtained from 6-wk old Swiss Webster mice (Charles River Breeding Laboratories Inc., Wilmington, MA) injected interperitoneally with 2 ml of thioglycolate 5 d before harvest. Cells were harvested by peritoneal lavage with ice-cold Hanks' balanced salt solution containing 10 U/ml of heparin and then centrifuged at 200 *g* for 10 min. The cells were washed twice in the same medium and then counted in a Coulter Counter (model Z_F, Coulter Electronics, Hialeah, FL). Cells were then diluted to 2–4 × 10^6 cells/ml in bicarbonate-free RPMI 1640 and kept in suspension in an end-over-end rotator. Peritoneal exudate cells were consistently >85% macrophages, as assessed by Wright's stain. The contaminating cells,

mostly lymphocytes, are not adherent and were therefore removed during plating before patch-clamping. Macrophage viability was >95%, as determined by exclusion of trypan blue.

Macroscopic pH Measurements

Intracellular pH was determined fluorimetrically using the pH-sensitive dye BCECF. Macrophages were loaded with BCECF by incubating 1×10^6 cells/ml with 2 μM of the parent acetoxymethyl ester for 10 min at 37°C followed by washing and resuspension in bicarbonate-free medium RPMI 1640. Before each measurement, the washed cells were sedimented and resuspended in the indicated solution. The fluorescence of thermostatted (37°C), magnetically stirred cell suspensions was measured in a Hitachi F-4000 fluorescence spectrophotometer, using excitation and emission wavelengths of 495 and 525 nm, respectively. Calibration of pH_i vs fluorescence intensity was preformed by the K^+-nigericin method of Thomas, Buchsbaum, Zimniak, and Racker (1979). The buffering power was determined using NH_4Cl pulses, as described by Roos and Boron (1981). Because the buffering power is nearly constant in the pH_i

TABLE I

Composition of Solutions

Solution	pH	Buffer	Salt	Acid/base
KCl-low β 6.5	6.5	10 MES	132.8 KCl	7.2 KOH
KCl-low β 7.5	7.5	10 HEPES	135 KCl	5 KOH
KCl 6.0	6.0	100 MES	75 KCl	44.1 KOH
KCl 6.5	6.5	100 MES	60 KCl	71.5 KOH
KCl 6.8	6.8	100 Pipes	25 KCl	100 KOH + 50 CsOH
KCl 7.5	7.5	100 HEPES	75 KCl	50 KOH
CsAsp 6.0	6.0	100 MES	75 CsAsp	44.1 CsOH
CsAsp 6.8	6.8	100 Pipes	25 CsAsp	150 CsOH
CsAsp 7.5	7.5	100 HEPES	75 CsAsp	50 CsOH
CsAsp 8.1	8.1	100 Tris	75 CsAsp	50 Aspartic acid
CsCl 7.5	7.5	100 HEPES	75 CsCl	50 CsOH
NMGAsp 7.5	7.5	100 HEPES	75 NMGAsp	50 N-methyl-D-glucamine

Concentrations are in mM. Unless otherwise specified, all media contained 1 mM $MgCl_2$ and 1 mM EGTA. When used for pipette filling, the media contained also 1 mM ATP. The osmolarity of all solutions was adjusted to 290 ± 5 mosM with the major salt.

range studied (A. Yi Qu, unpublished observations), the rates of change of pH_i reported in Fig. 1 are approximately proportional to the transmembrane H^+ (equivalent) flux.

Adherence, Visualization, and Perfusion for Single Cell Studies

For electrophysiological and microfluorimetric studies, suspended cells were plated on coverslips (25-mm diam, 10 oz, Red Label Micro Cover Glass, Thomas Scientific, Philadelphia, PA) that had been previously loaded into a Leiden Cover Slip Dish (Medical Systems Corp., Greenvale, NY). For plating, 0.5 ml of a macrophage suspension ($2–4 \times 10^5$ cells/ml RPMI 1640) was added to each dish and the cells were allowed 20–30 min at room temperature to adhere to the glass. The coverslips were then washed three times with bicarbonate-free RPMI 1640 to remove any nonadherent cells.

After adherence of the cells, the Leiden dish was placed into a holding chamber (Open Perfusion Micro-Incubator from Medical Systems Corp., Great Neck, NY) attached to the moveable stage of a Nikon Diaphot TMD inverted microscope (Nikon Canada, Toronto, ON).

Cells were visualized using a Nikon Fluor 40× oil-immersion objective and the Hoffman Modulation Contrast video system with angled condenser (Modulation Optics, Greenvale, NY), through a CCD-72 video camera and control unit (Dage-MTI) connected to a Panasonic monitor. The Micro-Incubator allows for constant perfusion of the cellular bath by attachment of perfusion tubes and the Leiden Aspirator. With a gravity driven system we maintained a perfusion rate of ≈0.5 ml/min, allowing for complete exchange of the bath solution once every minute. Each time the bath perfusate was changed, four complete bath exchanges (2 ml) were allowed before data collection was resumed.

Single Cell Fluorescence Ratio Determinations

For fluorescence measurements, the macrophages were incubated with 3 μM BCECF acetoxymethyl ester at a density of 1–2 × 10^6 cells/ml for 15 min at room temperature before adherence to the coverslip. Single cell fluorescence measurements were made using an M Series Dual Wavelength Illumination System from Photon Technologies Inc. (PTI, South Brunswick, NJ) in the dual-excitation-single-emission configuration. Excitation light was alternately selected using 495 ± 10 nm and 440 ± 10 nm filters at a rate of 100 Hz, then reflected at the cells by a 510-nm dichroic mirror. Light emitted by the cells was selected through a 520 nm long-pass filter. The emitted light and the red light (wavelength >600 nm) used for Hoffman imaging were separated with a 550 dichroic mirror. The fluorescence emission then traversed an infrared filter, an adjustable diaphragm (to isolate single cells) and a 530 ± 30 nm bandpass filter before reaching the photometer. Photometric data, recorded at a rate of 5 points/s were processed by the PTI software on an NEC 386 computer. Calibration of the fluorescence ratio vs pH was performed using the K^+/H^+ ionophore nigericin. Cells were perfused until equilibrated with K^+-rich (140 mM) media of varying pH that contained 5 μM nigericin. Calibration curves were constructed by plotting the extracellular pH (which is assumed to be identical to the internal pH; Thomas et al., 1979), against the corresponding fluorescence ratio. The resulting curve was sigmoidal with an inflection point ≈7.0, as expected from the reported pK_a of BCECF. When fluorescence measurements were acquired, the Hoffman illumination system was shuttered off to eliminate spurious signals generated by the red light.

Patch Clamping

The whole-cell configuration of the patch clamp technique was used to record ionic currents in macrophages, essentially as described by Hamill, Marty, Neher, Sakman, and Sigworth (1981). Patch electrodes were pulled from filament-filled borosilicate glass capillaries (World Precision Instruments, New Haven, CT) using a five-step protocol with a Brown and Flaming model P-87 horizontal puller (Sutter Instrument Co., Novato, CA). The resulting pipettes had resistances ranging from 10 to 20 MΩ as measured in the bath and were used without further polishing. Junction potentials were neutralized using the appropriate circuitry of the Axopatch-1D amplifier (Axon Instruments Inc., Foster City, CA). Cells were always patched in a stationary RPMI 1640 bath connected to the amplifier ground via an agar bridge (1% agar in 150 mM KCl). Successful pipette-to-cell attachments resulted in seal resistances varying from 10 to 50 GΩ, estimated using a Tektronix 2225, 50 MHz oscilloscope. Access resistance was monitored after break-in. Membrane input resistance in the whole-cell mode was found to range from ≈5 to 50 GΩ at normal pH_i. When applying maximal depolarizations to large, acid-loaded cells, the input resistance dropped to a minimum of ≈200 MΩ. Even in these extreme cases, the whole-cell resistance was at least 10-fold greater than the series resistance, when using the smallest pipettes (≈20 MΩ). Therefore, series resistance was not compensated. Bath perfusion with the appropriate solutions was initiated only after successful establishment of a patch. "Back-off" corrections for changes in junction potential due to dialysis of the cell interior after

attaining the whole-cell configuration (Barry and Lynch, 1991) were not applied, because they were independently estimated to be ≤ 6 mV and were often neutralized by changes of similar magnitude but opposite sign at the agar bridge junction.

The capacitance of the cells was found to range from 10 to 25 pF. Before data collection, the capacitance was compensated using the circuitry built into the patch clamp amplifier. To facilitate comparison between experiments, current traces were normalized using the capacitance determined for the corresponding cell. Currents in response to voltage steps or ramps were recorded using the Axopatch-1D amplifier in the voltage-clamp mode, coupled with a CV-4 1/100 headstage. Currents were filtered at 2 kHz with a four-pole Bessel filter and digitized on line at 3-ms intervals (unless indicated otherwise) using pClamp Clampex software (Axon Instruments Inc.) running on a Dell 386DX computer that interfaced with the amplifier by means of an analog-to-digital converter (TL-1 DMA Interface, Axon Instruments Inc.) and a LabMaster data acquisition board. Data analysis was carried out using pClamp Clampfit and Clampan (Axon Instruments Inc.) and Sigma Plot (Jandel Scientific, Corta Madera, CA) software. Leak current was determined by stepping the voltage from the holding potential of -60 mV to -90 mV in two 15-mV steps. When present, significant linear leak was subtracted from the current traces before analysis. All current records are shown with the convention that an upward deflection indicates outward current flow. Tail current amplitudes were determined by averaging the current in the 5–15 ms interval after termination of the conditioning pulse. Because the current did not deactivate sufficiently at positive voltages, currents recorded at negative potentials were mostly used for tail analysis.

It is generally assumed that the whole-cell patch configuration results in intracellular dialysis. Allowing for small Donnan-induced differences, the resulting ionic environment of the cytosol is expected to be essentially identical to that of the pipette solution. To ensure equilibration, at least 3 min were allowed between rupture of the membrane patch and the start of data collection. Adequate equilibration was confirmed by direct measurement of pH_i: using the calibration curve obtained in intact cells, the internal pH of cells patched in the whole-cell mode was virtually identical to the pH of the pipette filling solution (e.g., Figs. 2 and 3).

Other Methods

Permeability was calculated from the Goldman-Hodgkin-Katz current equation (Hille, 1992) using the nominal H^+ concentrations of the pipette and bath and assuming a specific capacitance of 1 $\mu F/cm^2$. Unless otherwise specified, all measurements were carried out at room temperature ($\approx 22°C$). Data are presented as representative traces of at least three similar experiments with cells from different animals or as means ± standard error (SE) of the number of experiments indicated.

RESULTS

Analysis of Cell Suspensions

The possible existence of a conductive H^+ permeability was assessed initially in suspensions of thioglycolate-elicited macrophages obtained from the peritoneal cavity of mice. The cytosolic pH was measured fluorimetrically using BCECF. To facilitate detection of the putative conductance, the activity of other H^+ (equivalent) transporting systems was minimized. For this purpose, the experiments were carried out in the nominal absence of Na^+ and HCO_3^-, to preclude Na^+/H^+ exchange as well as HCO_3^- exchange and cotransport. In addition, detection of the conductance was facilitated by increasing the protonmotive force. This was accomplished by acid-

loading of the cytosol using the ammonium prepulse technique (Roos and Boron, 1981). Finally, the K^+ conductive ionophore valinomycin was added to ensure that the counterion permeability would suffice to compensate the rheogenic movement of H^+ equivalents. As shown in Fig. 1 *A* (*top trace*), macrophages that were acid-loaded under these conditions tended to increase their cytosolic pH towards neutrality when suspended in a depolarizing (K^+-rich) solution, consistent with H^+ translocation across the plasma membrane through a conductive pathway. Considering the buffering power of macrophage cytosol, estimated to range between 20–25 mM/pH in the pH_i range studied (Swallow, Grinstein, and Rotstein, 1990), the maximal rates of H^+ extrusion through the putative conductance approach 9 meq/min/liter cells.

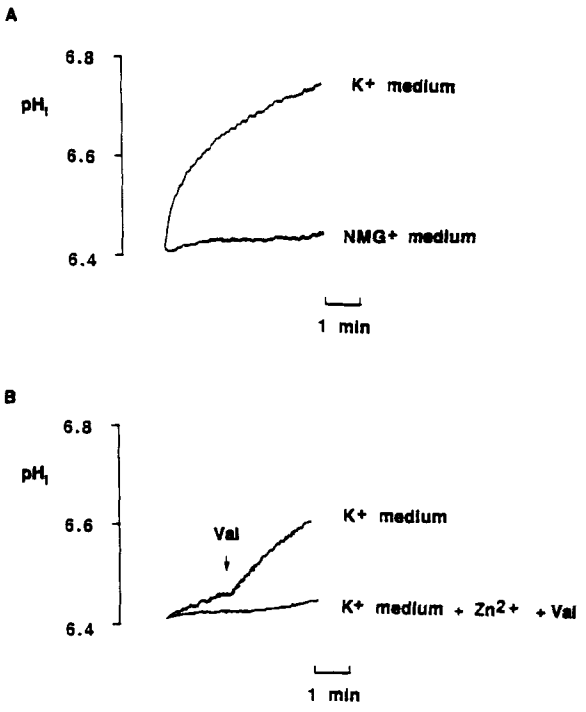

FIGURE 1. pH_i recovery of acid loaded macrophages. Macrophages were loaded with BCECF-AM and the pH_i of a population of suspended cells was measured as described under Materials and Methods. Before the initiation of the traces, the cells were preincubated in solution RPMI 1640 supplemented with 100 mM NH_4Cl for 20 min at 37°C. The recordings start immediately after resuspension of the cells in the indicated media at 37°C. (*A*) Top trace: K^+-medium; lower trace: NMG-medium. Both media contained 100 nM bafilomycin A_1 and 1 μM valinomycin. (*B*) Top trace: K^+-medium. Where indicated, 1 μM valinomycin (*Val*) was added. Lower trace: K^+-medium containing 1 μM valinomycin and 100 μM $ZnCl_2$ (Zn^{2+}). 100 nM bafilomycin A_1 was present in both traces. Traces are representative of at least three similar experiments with cells from different animals.

Earlier experiments examining pH_i recovery in acid-loaded peritoneal and alveolar macrophages demonstrated the existence of a vacuolar-type H^+ pump capable of proton extrusion (Swallow et al., 1988; Bidani, Brown, Heming, Gurich, and DuBose, 1989). The recovery noted in Fig. 1 *A*, however, cannot be attributed to such pumps, because this experiment was performed in the presence of bafilomycin A_1, a potent and selective inhibitor of vacuolar H^+ ATPases (Bowman, Siebers, and Altendorf, 1988). The concentration of bafilomycin used (100 nM) was several-fold greater than

required for inhibition of vacuolar H^+ ATPases in several systems, including murine macrophages (Bowman et al., 1988; Lukacs, Rotstein, and Grinstein, 1990).

Three lines of evidence suggest that the pH_i recovery described above is indeed mediated by a conductive pathway. First, the alkalinization was eliminated by suspension of the acid-loaded cells in an NMG^+-rich (low K^+) medium (Fig. 1 *A, lower trace*). Under these conditions, valinomycin tends to set the membrane potential (E_m) to an internally negative level, predicted to be ~ -85 mV, that does not favor net conductive H^+ efflux. Second, in K^+-rich medium the rate of H^+ extrusion is greater in the presence than in the absence of valinomycin (Fig. 1 *B, top trace*), suggesting that conductive counterion permeability is required and can limit the rate of translocation of H^+ equivalents. Finally, the pH_i recovery was blocked by extracellular Zn^{2+} (Fig. 1 *B, lower trace*), which was earlier reported to block H^+ conductive pathways in snail neurons (Byerly et al., 1984; Mahaut-Smith, 1989) and alveolar epithelial cells (DeCoursey, 1991). Taken together, these findings suggest that a comparable H^+ conductance exists in murine macrophages.

Analysis of Single Cells

Voltage-driven pH changes. While indicative of a H^+ (equivalent) permeability, the data obtained from fluorimetric pH_i determinations do not conclusively demonstrate that the pathway is conductive. In an attempt to confirm the rheogenic nature of the flux, and to gain further insights of its properties, we undertook simultaneous electrophysiological and fluorimetric analyses of single, adherent macrophages. The purpose of these experiments was to determine whether H^+ fluxes, measured as current and/or as pH_i changes, could be elicited by manipulating the transmembrane potential. Cells were patch-clamped in the whole-cell configuration with a pipette containing the free acid of BCECF (300 μM) dissolved in solution KCl-low β 6.5 (see Table I for details of composition of this and other media). The pH of this solution was 6.5, to approximate the conditions attained in the suspended, acid-loaded cells described above. The bathing medium was solution KCl-low β 7.5. After establishment of the whole-cell configuration, the cytosolic pH, determined from the fluorescence excitation ratio, equilibrated with the pH of the pipette within minutes. Under these conditions, when using a holding potential of −60 mV, pH remained stable over extended periods of time (Fig. 2, *leftmost column*). Voltage pulses of varying intensity were then applied for a period of 7 s while pH_i was monitored to assess the possible presence of conductive H^+ fluxes. No significant pH change was elicited by stepping the voltage to −30 mV, but a small (0.1–0.2 pH unit) yet reproducible intracellular alkalinization was recorded at 0 mV, consistent with the results obtained in cells suspended in K^+-rich medium containing valinomycin (Fig. 1). The pH_i increase became more pronounced at progressively more depolarizing voltages (Fig. 2). At +60 mV, a massive alkalinization of nearly 1 pH U developed during the 7-s pulse. It is noteworthy that these pH changes occurred despite the continuity between the cytosolic compartment and the internal pipette solution, which was buffered to pH 6.5 with 10 mM MES. Thus, under the conditions used, the voltage-driven transmembrane movement of acid equivalents outstrips the diffusion of buffer from the pipette. After termination of the depolarizing pulse, pH_i returned towards its initial value, most likely the result of diffusion of buffer from the pipette

to the cell interior. This is better appreciated in the expanded time scale illustrated in Fig. 3 *A*.

The amount of acid equivalents translocated during the voltage pulse can be estimated from the rate of pH change and the buffering power. While precise values for the latter cannot be established, upper and lower limits can be defined. The buffering power of the cytosolic compartment of the patched cell must be greater than that of the pipette solution ($\approx$4 mM/pH at pH 6.5) but smaller than the sum of

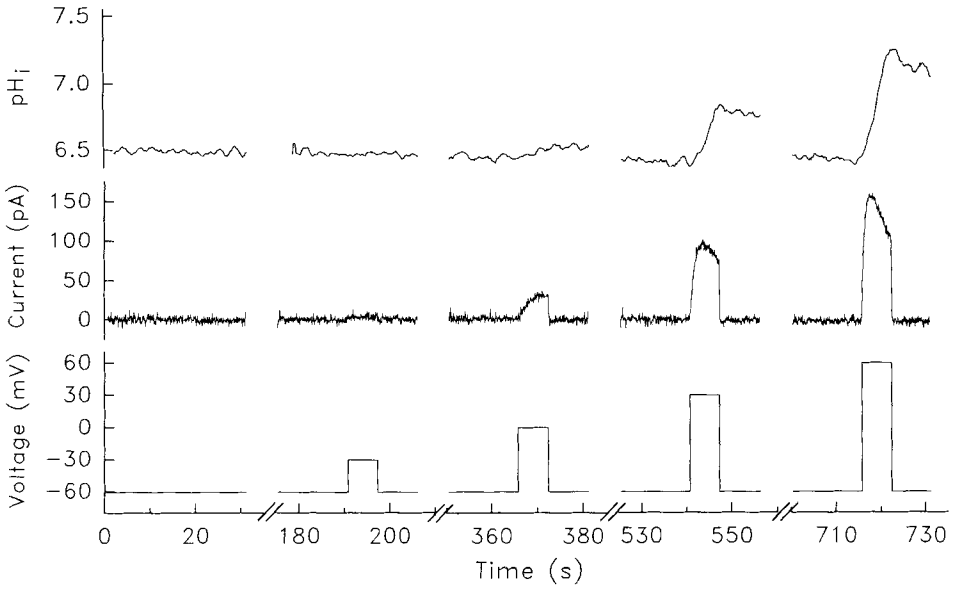

FIGURE 2. Depolarization increases pH_i and activates an outward current. BCECF-loaded macrophages were plated on a glass coverslip and patched in the whole-cell configuration at a holding voltage of −60 mV. The patch pipette contained solution KCl-low β 6.5 (see Table I for composition of this and other media) supplemented with 300 μM BCECF (free acid) and 1 mM MgATP and had a 20 MΩ resistance, and the bath was continually perfused with solution KCl-low β 7.5. Cells were then subjected to voltage steps lasting 7 s, at 180 s intervals. The voltage protocol is illustrated by the bottom traces. The corresponding whole cell currents are illustrated in the middle traces. pH_i was estimated simultaneously in the patched cell by measuring the fluorescence ratio of BCECF, and is shown by the top traces. The capacitance of the cell illustrated was 15.9 pF. Data are representative of four similar experiments using cells from different mice.

the buffering power of the cytosol of intact cells ($\approx$25 mM/pH) plus that of the pipette solution. Thus, in the experiment illustrated in Fig. 2, between 2×10^8 and 12.5×10^8 H^+ equivalents traversed the membrane per s at +60 mV. This charge flow is equivalent to 32–200 pA, a current that should be readily detectable by electrophysiological means. In agreement with this prediction, an outward current was found to accompany the voltage-driven pH changes. The current was marginal at −30 mV, but increased markedly at more positive potentials (see middle traces in

Fig. 2), exceeding 150 pA at +60 mV. Comparison with the value predicted above on the basis of the pH change suggests that a sizable fraction of the current is carried by H^+ equivalents. In support of this notion, the voltage dependence of the current and of the pH changes were found to be very similar. While current and net H^+

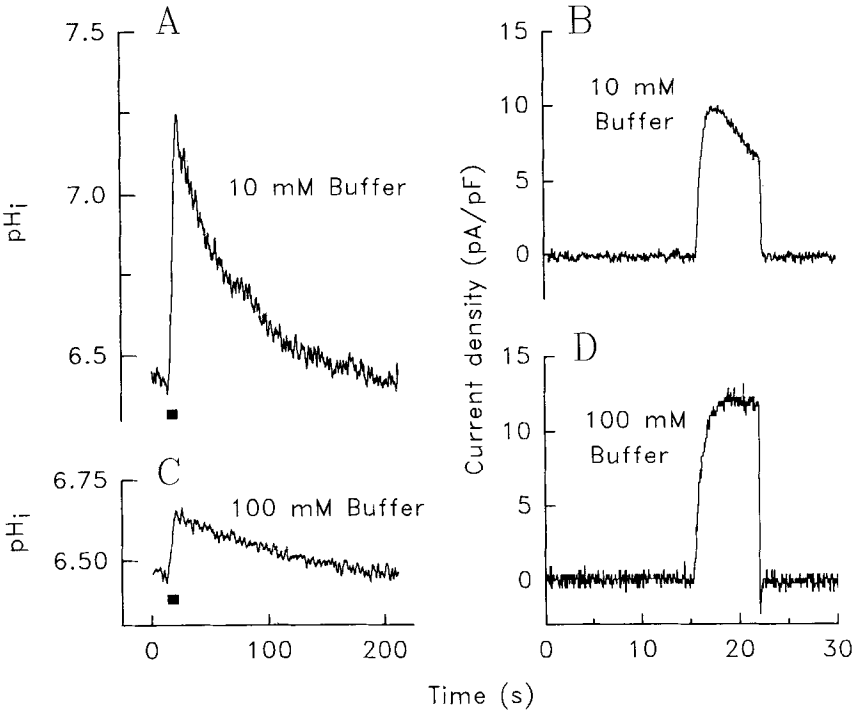

FIGURE 3. Effect of the buffering power on the voltage-induced pH_i changes and associated current. Adherent BCECF-loaded macrophages were patched in the whole-cell configuration and clamped at a holding voltage of −60 mV. The patch pipette was loaded with either solution KCl-low β 6.5 (*A* and *B*) or with solution KCl 6.5 (*C* and *D*) supplemented with BCECF and ATP as in Fig. 2. The buffer (MES) concentrations of these solutions are indicated. The bath was continually perfused with either solution KCl-low β 7.5 (*A* and *B*) or KCl 7.5 (*C* and *D*). 15 s after initiation of the traces, the voltage was driven to +60 mV for 7 s. This period is indicated by the solid bars in *A* and *C*. Intracellular pH_i (*A* and *C*) and current (*B* and *D*) were measured simultaneously as described for Fig. 2. The capacitance of the cells illustrated in *A* and *B*, and *C* and *D* were 15.9 and 15.5 pF, respectively. Pipettes of similar size (≈20 MΩ) were used for both cells. The current measurements were normalized per cell capacitance and are displayed as current density (pA/pF) to allow for comparison between cells. While current measurements ceased soon after the voltage pulse, pH_i measurements were continued until a return to pre-pulse conditions was observed. Data are representative of at least three experiments using cells from different mice.

translocation are not detectable below −30 mV, an intracellular alkalinization and the outward current develop in parallel at more positive potentials (Fig. 4).

Optimizing the experimental conditions for current measurement. A more detailed analysis of the current was required to establish its relationship to H^+ translocation.

For this purpose, maintenance of constant ionic conditions throughout the experimental protocol is necessary. It was therefore essential to minimize the pH changes that accompany the application of current. To circumvent this difficulty, the experiments described hereafter utilized pipette solutions with very high buffering power (100 mM of an organic buffer with pK identical to or very near the experimental pH). As shown in Fig. 3, application of comparable depolarizing pulses to cells of similar size perfused internally with media of varying buffering power resulted in markedly different pH transients (cf 3, *A* and *C*), as expected. It was our impression that the current associated with these transients, normalized per unit area (capacitance), was greater and more stable at high buffering power (Fig. 3, *B* and *D*). When applying pulses of 30 mV, the peak current density in two experiments was 12.5% greater at high buffering power and the current was 62% greater at 7 s. At 60 mV, the average currents using high buffer were 26 and 69% greater at the peak and at 7 s,

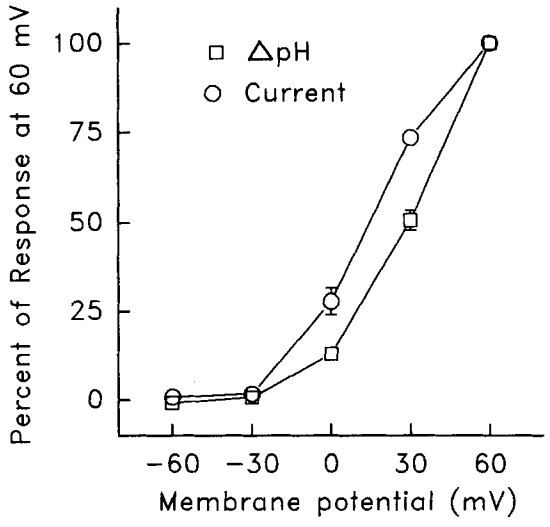

FIGURE 4. Parallel development of outward current and H^+ (equivalent) efflux with membrane depolarization. The voltage-induced currents and pH_i changes were measured in experiments like that illustrated in Fig. 2. Maximal currents (*circles*) and pH changes (*squares; ΔpH*) recorded during the 7-s depolarizing pulse were measured in four similar experiments. To allow comparison, data were normalized as percentage of the response obtained at +60 mV. Data are means ± SEM of four experiments. Where absent, error bars were smaller than the symbol.

respectively. The mechanism and significance of this finding is discussed in detail below.

Two other measures were taken in an attempt to ensure that comparable pH prevailed at all times during the course of current-voltage analyses. First, the duration of the pulses was minimized, sometimes at the expense of not attaining current equilibration for a given voltage. Second, long intervals at the holding potential were allowed between pulses, to enable diffusion of buffer from the pipette into the cell to restore the initial pH (e.g., Fig. 3). The duration of these intervals (usually 30 s) was limited by the stability and survival of the whole-cell preparation. Under most conditions, this choice of parameters effectively stabilized the internal pH. Nevertheless, a small yet significant alkalosis ($\leq$0.2 pH U) was observed when succesive large currents were applied, possibly accounting for some of the observations described below.

Current-voltage relationship. The voltage protocol used for analysis of the outward current is illustrated in the bottom left panel of Fig. 5. The holding potential was −60 mV. Pulses lasting 2.5 s were applied between −90 and +75 mV at 15 mV increments. The internal pH was stabilized at 6.5 with 100 mM MES. As illustrated in

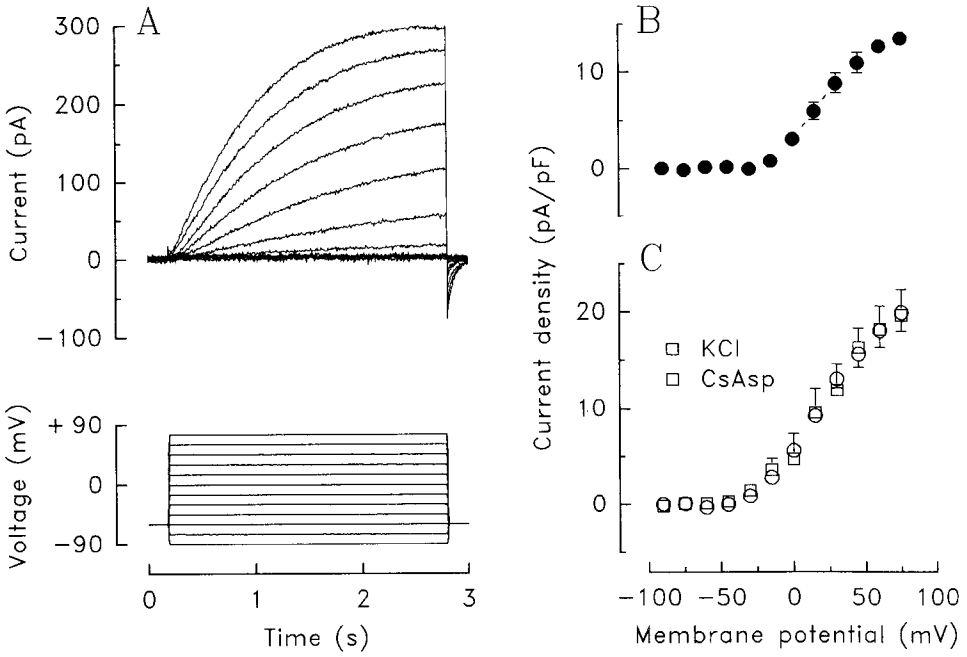

FIGURE 5. Current-voltage relationship. Adherent macrophages patched in the whole-cell configuration were clamped at a holding potential of −60 mV. (*A–B*) The pipette (10 MΩ) contained solution KCl 6.5 with 1 mM MgATP and the bath was perfused with solution KCl 7.5. Pulses lasting 2.5 s were applied between −90 and +75 mV in 15 mV increments at 30-s intervals, as illustrated by the voltage protocol shown in the bottom left panel. (*A*) Representative family of currents elicited from a single cell with 20.5 pF capacitance by application of the voltage protocol. (*B*) Current-voltage relationship. Points were calculated by averaging the current during the last 150 ms of each voltage pulse. The currents of three cells from different animals were normalized per cell capacitance and are plotted vs the applied potential. Values are means ± SEM (n = 3). (*C*) The voltage protocol illustrated in *A* was applied to cells patched under two different ionic conditions. (*Squares*) Pipette solution was KCl 6.0 with 1 mM ATP, bath solution was KCl 7.5. (*Circles*) Pipette solution was CsAsp 6.0 with 1 mM ATP, bath solution was CsAsp 7.5. The current was normalized per capacitance as in *B*. Data are means ± SEM of three cells from different experiments. SE bars are upward for KCl and downward for CsAsp. Where absent in *B* or *C*, bars were smaller than symbol.

Fig. 5 *A*, little current was detectable at potentials below −15 mV, but a distinct outward current was recorded at this and more positive potentials. The current activated slowly, often with sigmoid kinetics which were more apparent at low voltages. A more detailed account of the activation kinetics is presented below. In

contrast, deactivation upon restoration of the holding potential (−60 mV) was rapid ($t_{1/2} \approx 45$ ms when the conditioning pulse was +60 mV) and could be adequately fitted by a single exponential.

The average current-voltage relationship of three cells is presented in *B* of Fig. 5. To facilitate comparison between cells of different size, the current has been normalized per unit membrane capacitance and is presented as current density (pA/pF). As is apparent from the scatter of the data in this and subsequent figures, the current magnitude was closely related to the size of the cells, as estimated from the capacitance (range 10–25 pF), validating the normalization procedure. The current, which is negligible below −15 mV, increases sharply at more positive voltages, reaching 13 pA/pF at +75 mV. More positive voltages were not explored, as they induced instability of the seal.

In these and all other experiments illustrated in the figures, 1 mM ATP was present in the pipette solution. However, very similar results were obtained in the absence of the nucleotide, suggesting that the currents recorded are ATP-independent.

Ionic substitution. The experiments shown in Figs. 2–5 *B* were performed in bilateral KCl solutions. While movement of H^+ equivalents was estimated to be a substantial component of the current, the contribution of other species was not delineated. Ionic substitution experiments were therefore undertaken to define the relative contribution of the different ionic species to the outward current. A typical experiment is shown in Fig. 5 *C*. Intracellular pH was buffered at 6.0 to maximize the outward flux of H^+ equivalents. As before, little current was noted in bilateral KCl at or near the holding voltage, but outward current appeared at more positive potentials. A similar analysis was performed in cells bathed in bilateral Cs-aspartate (CsAsp). This condition (solution CsAsp 6.0 in the pipette and CsAsp 7.5 in the bath) minimizes the possible permeation of the major ionic constituents of the medium, since aspartate, MES (the internal pH buffer) and HEPES (the external buffer) are thought to be too large to permeate anion channels, while Cs^+ not only fails to traverse most cation channels, but is also an effective K^+ channel blocker. Remarkably, the current recorded in CsAsp was virtually identical to that in KCl. Similar results were obtained bathing the cells in solution CsCl 7.5 or in NMGAsp 7.5. This might suggest that the underlying conductance is extremely nonselective, unable to discern between the substituents used or, more likely, the data may indicate that an ionic species other than the major constituents of the medium carries the outward current. Our failure to detect the voltage-gated K^+ or Cl^- currents reported to exist in macrophages (see Gallin, 1991 for review) is probably due to an inhibitory effect of the low intracellular pH used in these experiments.

Tail current analysis. The reversal potential of tail currents was used to identify the ionic species responsible for the outward current. The conductance was initially activated by the application of a depolarizing pulse. The magnitude and duration of this conditioning pulse was limited to minimize changes in intracellular pH, which could conceivably affect the properties of the tail currents. Test pulses of varying voltage were then applied and the deactivating currents were recorded. A typical voltage protocol is illustrated in the middle panel of Fig. 6 and the associated currents are shown in the top panel of Fig. 6 *A*. The voltage dependence of the tail

currents, determined in the 5–15 ms interval after imposition of the test voltage, is summarized in Fig. 6 *B*. Unlike the steady state or peak current-voltage curves, the instantaneous current-voltage relationship was nearly linear. The slight nonlinearity could be accounted for by a faster deactivation at more negative potentials or to asymmetric distribution of the transported species. Because KCl was the primary salt on both sides of the membrane, Goldman-Hodgkin rectification would not be

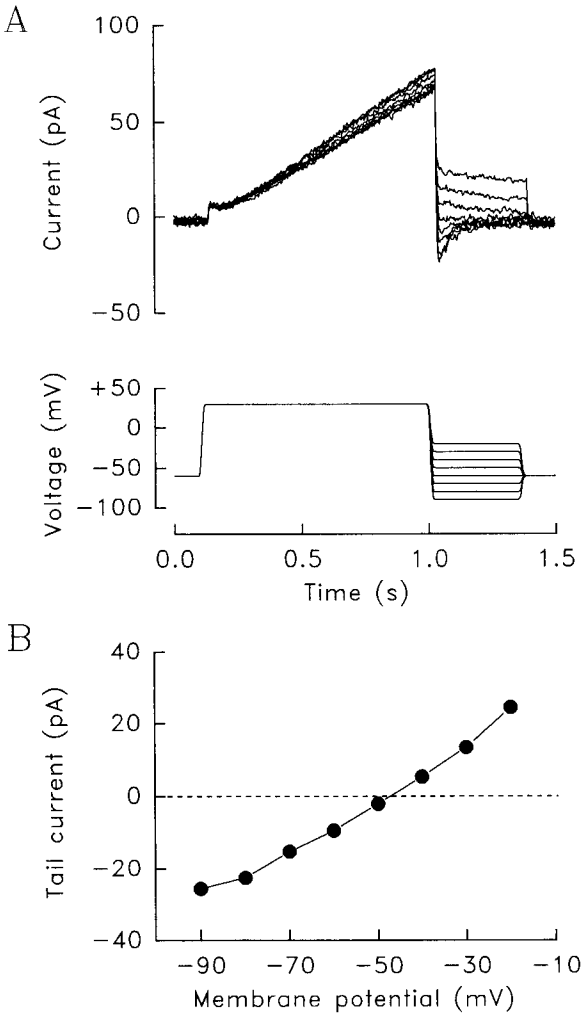

FIGURE 6. Determination of reversal potential of tail currents. Adherent macrophages were patched in the whole-cell configuration with a pipette of 12 MΩ filled with solution KCl 6.5 with 1 mM ATP and perfused externally with solution KCl 7.5. The holding potential was −60 mV. Outward current was first activated by a 900 ms depolarizing pulse to +30 mV. Test pulses lasting 350 ms were next applied between −90 and −20 mV in +10 mV increments, as illustrated by the voltage protocol in the middle panel. (*A*) Composite illustrating representative currents obtained from a cell of 16.2 pF. (*B*) Voltage dependence of the tail currents, averaged in the 5–15 ms interval after the start of the test pulse. Data are representative of three similar experiments under the ionic conditions specified. Dashed line is zero current level, used to determine E_{rev} (see legend to Fig. 7).

anticipated a priori, unless minor species such as H^+, which are asymmetrically distributed, contribute predominantly to the current.

The reversal potential of the tail current (E_{rev}) was determined from the intercept of curves like that shown in Fig. 6 *B*. Clearly, E_{rev} in the experiment of Fig. 6 (≈ -50 mV) is considerably more negative than predicted for either K^+ or Cl^-, the major ionic constituents. This discrepancy persisted when cells were bathed bilaterally with

TABLE II

Reversal Potential of Tail Currents

Ions		KCl	CsCl	CsAsp	NMGAsp	E_H
		pH 7.5				
KCl,	pH 6.0	−70.12 ± 7.90	−68.22 ± 8.23	−71.92 ± 5.32	−63.25 ± 9.88	−87.0
CsAsp,	pH 6.0	−68.92 ± 1.63	−58.34 ± 6.12	−69.17 ± 9.25*	−59.00 ± 4.22	
KCl,	pH 6.8	−38.99 ± 1.47	−42.26 ± 2.96	−33.78 ± 5.19	−36.83 ± 2.43	−40.6
CsAsp,	pH 6.8	−33.47 ± 4.26	−39.90 ± 6.18	−38.07 ± 3.60*	−34.05 ± 3.52	

Adherent macrophages were patched in the whole-cell mode with pipettes filled with the solutions listed in the leftmost column, at the indicated pH (second column; see Table I for detailed solution composition). The composition of the external solution is given by the headings of the remaining columns. The bath pH was always 7.5. Reversal potentials were calculated from the tail currents as described for Fig. 6. E_{H^+} is the proton equilibrium potential calculated for the two pH gradients examined, at room temperature (rightmost column). Data are in mV and represent the mean ± SEM of three experiments except when indicated by the asterisk, where n = 6.

CsAsp (Table II). Moreover, E_{rev} was virtually unaffected by imposition of large inward or outward K^+ or Cl^- gradients (see Table II). Ca^{2+} and Mg^{2+} are similarly unlikely to account for the anomalous E_{rev}, because Ca^{2+} was nominally absent and Mg^{2+} was symetrically distributed. Instead, E_{rev} approximated the equilibrium

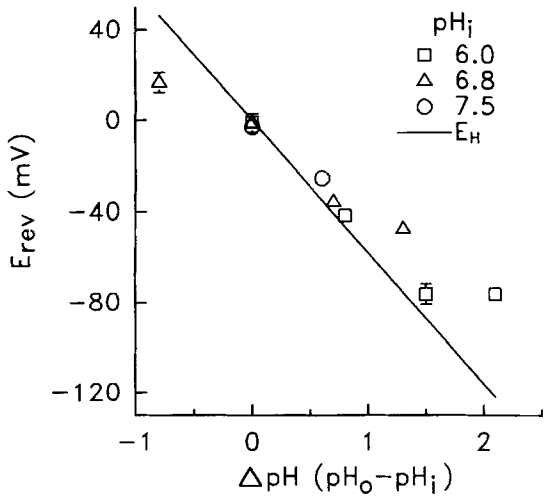

FIGURE 7. Relationship between the reversal potential of tail currents and the transmembrane pH gradient. Adherent macrophages were patched in the whole-cell configuration. Patch pipettes were filled with solution CsAsp 6.0 (*squares*), CsAsp 6.8 (*triangles*) or CsAsp 7.5 (*circles*), containing 1 mM ATP. The following bath solutions were tested for each pipette type: CsAsp 6.0, CsAsp 6.8, CsAsp 7.5, CsAsp 8.1. Reversal potentials were determined using a protocol like that described in Fig. 6. Depolarizing conditioning voltages, chosen to activate the current yet minimize pH_i changes, ranged from 0 mV at ΔpH = 2.1 to +110 mV at ΔpH = −0.8. Test pulses started as low as −120 mV (for ΔpH = 2.1) and increased in 10-mV steps to a maximum at least 40 mV negative to the voltage of the conditioning pulse. Linear regression of 2–3 points on either side of the zero current level was used to calculate E_{rev}. Other points were omitted from the calculation to obviate problems with Goldman-Hodgkin rectification and/or voltage induced differences in the rate of inactivation. E_{rev} is plotted vs the ΔpH, calculated as the difference between the extra- and intra-cellular pH. Positive values indicate relative internal acidity. Each point represents the mean ± SEM of three experiments using cells from different animals. Where absent, error bars were smaller than the symbol. The solid line is the predicted H^+ equilibrium potential (E_{H^+}).

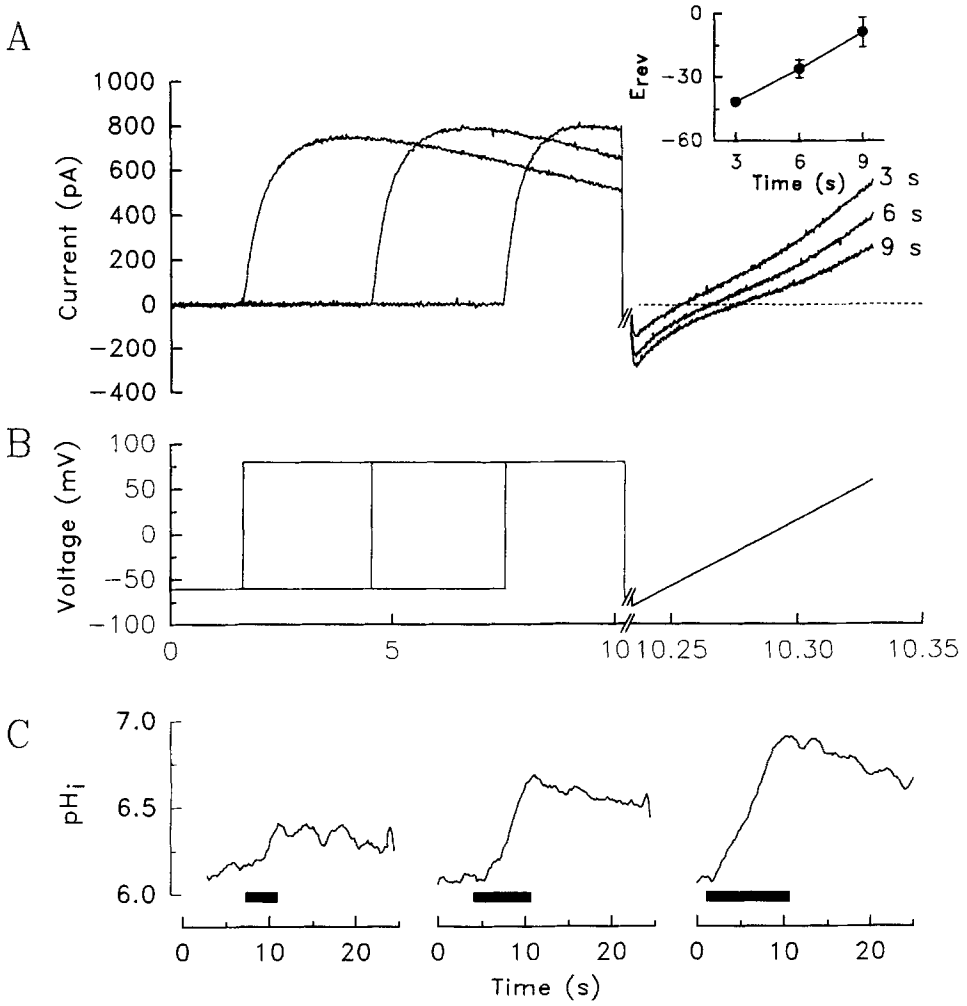

FIGURE 8. Apparent inactivation of H^+ conductance. BCECF-loaded macrophages were plated on a glass coverslip and patched in the whole-cell configuration at a holding voltage of −60 mV. The patch pipette contained solution CsAsp 6.0 supplemented with 300 μM BCECF (free acid) and 1 mM MgATP, and the bath was continually perfused with solution CsAsp 7.5. Where indicated, a depolarizing pulse to +80 mV was applied for either 3, 6, or 9 s, as illustrated by the voltage protocol in *B*. Immediately after the depolarizing pulse, the cells were subjected to a voltage ramp from −80 mV to +60 mV over a 100-ms period (see *B*; notice change in time scale at break). 2-min intervals at the holding voltage were allowed between measurements, to promote recovery of the initial pH. Data were acquired at 50 Hz during the square pulse and at 5 kHz during the ramp. Pipette resistance was 10 MΩ. Cell capacitance was 19.7 pF. (*A*) Composite illustrating currents. The *inset* in *A* illustrates the dependence of E_{rev}, calculated from the zero-current measured during the voltage ramp, on the duration of the depolarizing pulse (abscissa; in s). The data in the inset are the means ± SEM of four experiments. (*C*) pH_i changes during application of depolarizing pulses. pH_i was measured with BCECF simultaneously with the current determinations during application of the 3 s (*left trace*), 6 s (*middle trace*), and 9 s (*rightmost trace*) voltage pulses. The period of voltage application

potential predicted for H^+ (E_{H^+}; see last column of Table II). These findings provide a strong indication that H^+ (equivalents) are the species primarily responsible for the voltage-dependent outward currents in acid-loaded cells.

To confirm this notion, the ΔpH dependence of E_{rev} was analyzed. Cells were patched in the whole-cell configuration with pipettes containing CsAsp solutions buffered to pH 6.0, 6.8 or 7.5 (see Table I for detailed composition). E_{rev} was determined at varying external pH levels in CsAsp media and the results are summarized in Fig. 7. A very good correlation exists between ΔpH and E_{rev}, particularly when moderate gradients were imposed. Significant departures from the predicted E_{H^+} (*solid line,* Fig. 7) were observed when the cells were subjected to more extreme ΔpHs. It is noteworthy that the good correlation between E_{rev} and E_{H^+} was applicable at varying pH_i levels (Fig. 7) and persisted when the primary ionic constituents were randomly substituted (Table II). Together, the data in Figs. 2–7 indicate that the voltage-sensitive outward current is carried primarily, if not entirely by H^+ equivalents. While OH^- or other acid equivalents could in principle be the transported species, the current will be attributed hereafter to a H^+ conductance, for simplicity.

Apparent inactivation of the H^+ conductance. As shown in Fig. 2, prolonged application of depolarizing pulses resulted in a gradual decrease of the associated current, suggesting the occurrence of inactivation. This phenomenon is more clearly illustrated in Fig. 8, where the effects of depolarizing steps of increasing duration are compared. At the voltage used, activation of the conductance was complete after 1–2 s, but a progressive decrease of the current was noticeable shortly thereafter. This inactivation was barely apparent after 3 s and increased gradually throughout the 9-s period studied (Fig. 8 *A*).

Inactivation, in the conventional sense, refers to a time- and/or voltage-dependent decrease in conductance (Hille, 1992). To establish whether the decreased current in Fig. 8 was attributable to a progressive decrease in the H^+ conductance, the current-voltage relationship was studied by applying a voltage ramp immediately after conditioning depolarizing pulses of varying length (see Fig. 8 *B* for voltage protocol; notice change in time scale after break). Contrary to our expectation, the instantaneous inward current following a prolonged depolarization was greater than that observed after short pulses (Fig. 8 *A*). This finding implies that factors other than a reduced conductance must have contributed to the apparent inactivation of the outward H^+ current.

An indication of the mechanism underlying the inactivation was obtained from determinations of the reversal potential of the current following pulses of increasing duration. E_{rev}, given by the intercept of the current ramps with the dotted (zero current) line in Fig. 8 *A*, displayed a progressive positive shift at longer times. The relationship between E_{rev} and the duration of the conditioning pulse is summarized in the inset of Fig. 8 *A*. Because protons were identified earlier as the transported

---

is indicated by the solid bars. Note that the time scale differs from that in *A* and *B*. The current and pH traces correspond to a single experiment representative of four. Apparent inactivation of the current, shifts in the reversal potential and intracellular alkalinization were recorded in all cases.

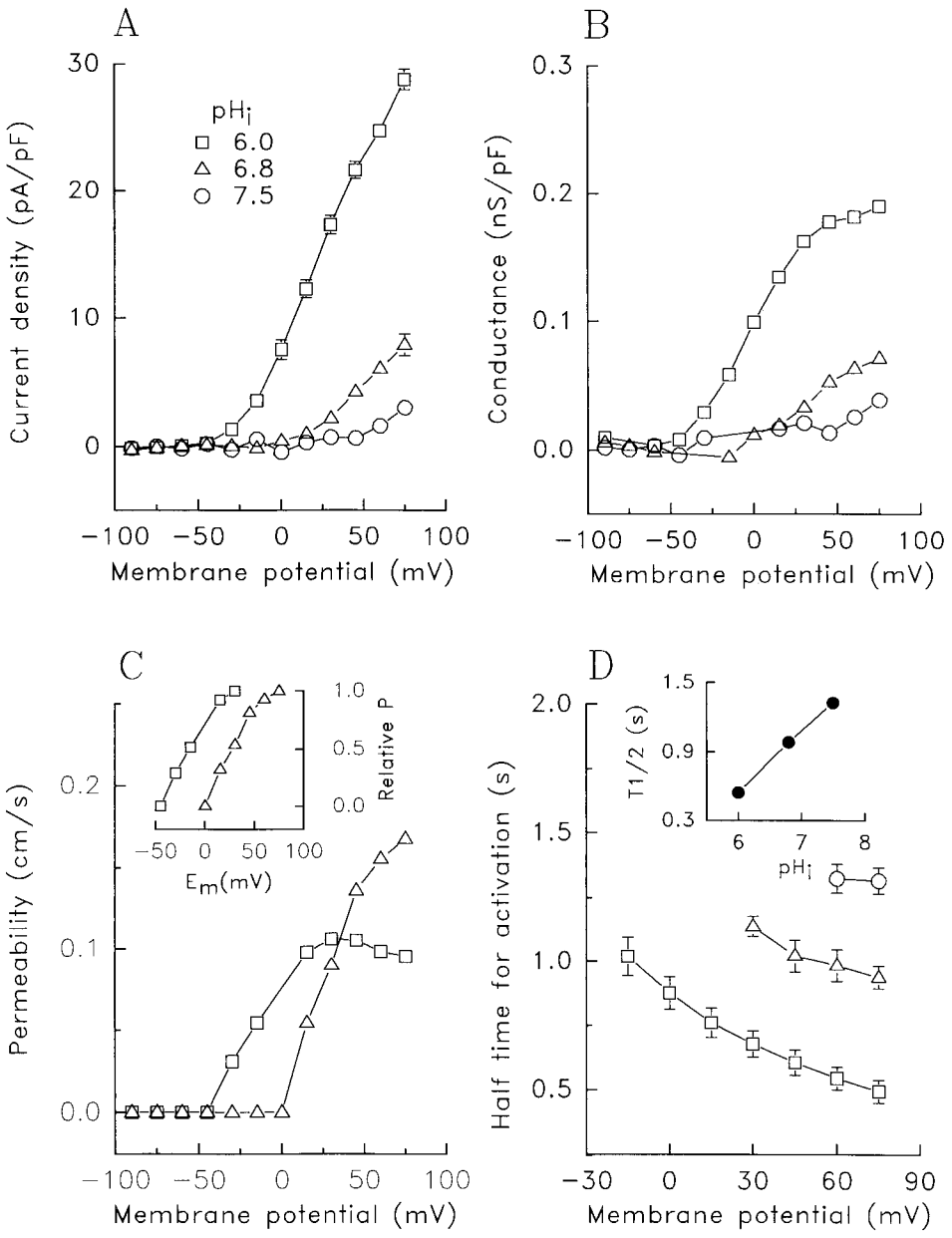

FIGURE 9. Effect of pH_i on H^+ conductance. Adherent macrophages were patched in the whole-cell mode with pipettes containing one of the following solutions: CsAsp 6.0 (*squares*), CsAsp 6.8 (*triangles*), or CsAsp 7.5 (*circles*). The bath solution was CsAsp 7.5 in all cases. (*A*) Current-voltage relationships, generated using the protocol described in Fig. 5. Currents were normalized per capacitance. The data are means ± SEM of three experiments. Where absent, error bars were smaller than the symbol. (*B*) Conductance vs voltage relationship determined using the mean values from *A* and the calculated E_{rev}, as described in the text. The chord conductance was not estimated within 15 mV of the calculated E_{rev}, a range where the deter-

species, a sizable change in the transmembrane ΔpH must have occurred to account for the shift in E_{rev}. This prediction was borne out by direct measurement of intracellular pH. As illustrated in Fig. 8 *C*, a significant cytosolic alkalinization was detectable even after 3 s. The pH change was more pronounced with longer pulses, approaching 0.8 U after 9 s. Assuming that the external pH remained constant, the measured internal alkalinization can largely account for the positive displacement of E_{rev}. The pH change is much more apparent in Fig. 8 *C* than in Fig. 3 *C*, despite the use of comparable buffer concentrations. This is due to the greater (≈ fourfold) current density in the experiment of Fig. 8 *C*, resulting from the lower initial pH and more positive voltage applied.

The intracellular pH changes that develop during current application, together with possible changes in the pH of the extracellular unstirred layer, are likely to account for the apparent inactivation of the outward current by changing the protonmotive force. Consistent with this interpretation, the outward current density is greater and more sustained when using higher buffering power in the pipette (cf Fig. 3, *B* and *D*), presumably by reducing the pH_i changes associated with the voltage pulse (Fig. 3, *A* and *C*). In view of these results, the inactivation of the current does not appear to reflect an intrinsic property of the conductive pathway. Instead, the progressive inhibition seemingly results from decreasing force for outward H^+ translocation. Direct effects of varying pH_i on H^+ conductance are also possible and are discussed in detail below.

Effect of pH_i on H^+ conductance. Fig. 9 *A* shows current-voltage relationships of cells clamped with pipettes containing CsAsp solutions of varying pH. The pH of the extracellular solution was the same (7.5) in all cases. Two main features are apparent: (*a*) the threshold for activation of the current is lower (more negative) at lower intracellular pH; and (*b*) the steepness of the curves decreases as pH_i is increased. To define if the latter effect is due exclusively to the change in protonmotive force or whether pH_i alters the H^+ conductance, the chord conductance was estimated and is plotted in Fig. 9 *B*. Chord proton conductance (G_{H^+}) was calculated as:

$$G_{H^+} = I_{H^+}/(E_m - E_{rev}),$$

where I_{H^+} is the measured current and E_{rev} was the reversal potential calculated from the tail current analysis. As is apparent from Fig. 9 *B*, the conductance was a function of the transmembrane potential, displaying a sharp threshold followed by an approximately linear increase phase and attaining near saturation when sufficiently

---

minations are inherently inaccurate. (*C*) Permeability vs voltage relationship calculated from the mean values in *A* and the nominal pH_i (pipette solution pH) and pH_o, using the Goldman-Hodgkin-Katz current equation. Only the data at pH_i 6.0 and 6.8 are presented. The small current and low $[H^+]$ at pH_i 7.5 make the calculations unreliable. (*Inset*) Relative permeability vs voltage plot. Permeability (*P*) was normalized to the maximum value at each pH, even if saturation was not reached. (*D*) Voltage dependence of the time required for half-maximal activation of the current. Maximal current was defined as that measured at the end of the 2.5 s depolarizing pulse. Data are means ± SEM of three separate experiments. (*Inset*) pH_i-dependence of the time for half-maximal activation, plotted using the mean values in *D* determined at +60 mV.

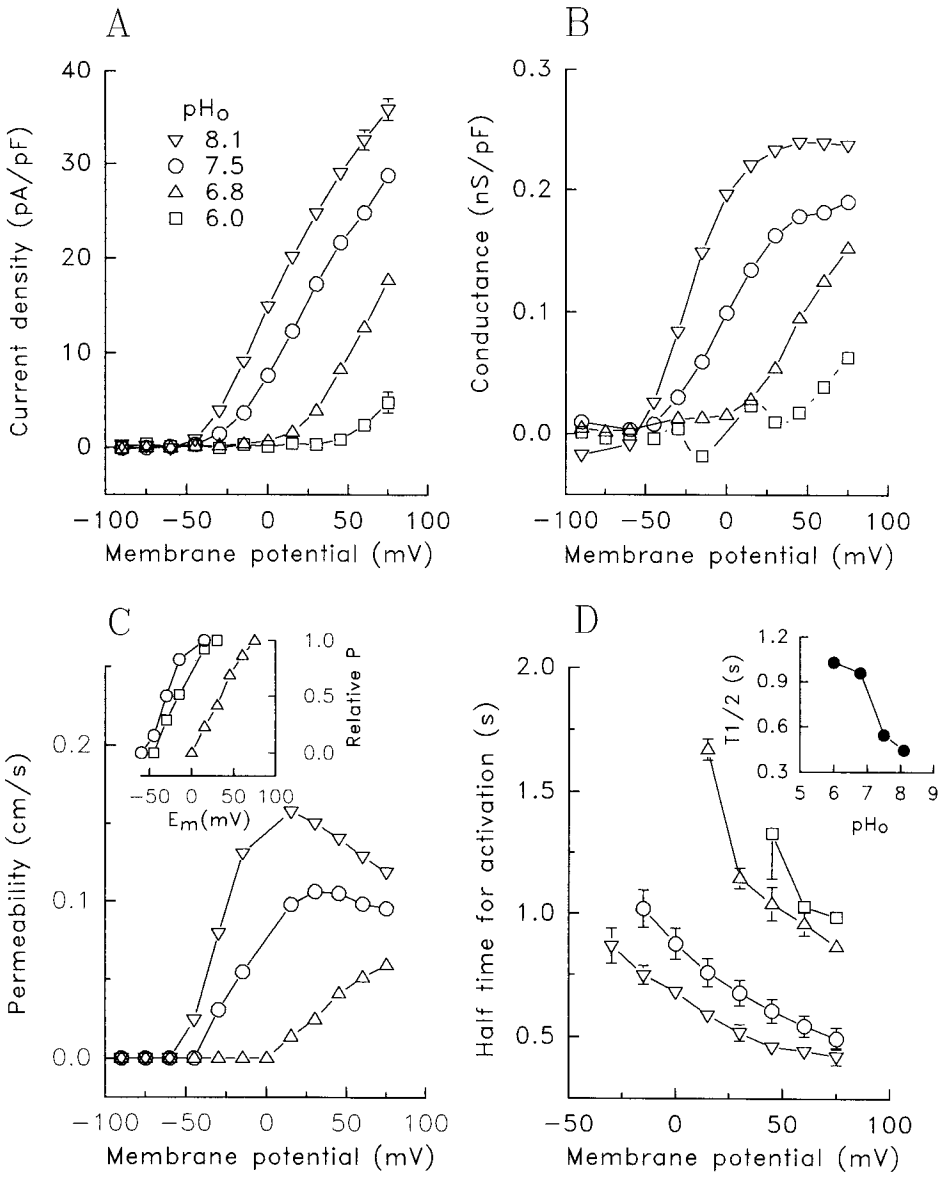

FIGURE 10. Effect of pH_o on H^+ conductance. Adherent macrophages were patched in the whole-cell mode with pipettes filled with solution CsAsp 6.0. The bath solution was CsAsp 6.0 (*squares*), CsAsp 6.8 (*triangles*), CsAsp 7.5 (*circles*) or CsAsp 8.1 (*inverted triangles*), as indicated. (*A*) Current-voltage relationships, generated using the protocol described in Fig. 5. Currents were normalized per capacitance. The data are means ± SEM of three experiments. Where absent, error bars were smaller than the symbol. (*B*) Conductance-voltage relationship determined using the mean values from *A* and the calculated E_{rev}, as described in Fig. 9. (*C*) Permeability vs voltage relationship calculated from the mean values of A and the nominal pH_i (pipette solution pH) and pH_o, using the Goldman-Hodgkin-Katz current equation. Only the data at pH_o 6.8–8.1 are presented. (*Inset*) Relative permeability vs voltage plot. Permeability (*P*)

positive voltages were reached. At pH_i 6.0 the conductance was half-maximal near 0 mV and reached apparent saturation at a level of $\approx$0.2 nS/pF around +50 mV. Importantly, the conductance is not solely a function of the transmembrane potential, but of the internal pH as well. Increasing pH_i shifted the threshold voltage for activation of the conductance to more depolarized levels.

The magnitude of the conductance is determined in part by the availability of the charge carrying species, i.e., by the H^+ (equivalent) concentration. To more directly assess the effects of voltage and pH on the activation of the transport pathway, permeability was calculated from the current and pH values, using the Goldman-Hodgkin-Katz current equation and assuming a specific capacitance of 1 $\mu F/cm^2$. The resulting data are plotted in Fig. 9 *C* as a function of membrane potential. Because calculation of permeabilities at the low $[H^+]$ and small currents observed at pH_i 7.5 is inaccurate, only the data obtained at pH 6.8 and 6.0 are presented. The results indicate that the shift in the activation threshold cannot be attributed to changes in substrate ion concentration and must, instead, reflect a pH dependent alteration in the behavior of the permeation pathway. At pH 6.8, the permeability increases throughout the voltage range studied, reaching 0.17 cm/s at +75 mV. In contrast, at pH 6.0, the permeability appears to saturate at a maximal level of $\approx$0.11 cm/s. While this apparent saturation may be a valid reflection of the behavior of the permeation pathway, it is likely to be dictated, at least in part, by differences between the theoretical pH used for the calculation (that of the pipette solution) and the true pH prevailing at the internal face of the membrane after application of a series of current pulses (see page 747 for discussion of this effect). In other words, the permeability at the highest voltages may have been underestimated due to depletion of the charge carrying species, i.e., H^+ equivalents. The steepness of the activation curve appears to be similar at pH 6.0 and 6.8, which is more apparent when the data are normalized to the maximal permeability recorded at each pH (inset Fig. 9 *C*).

The change in the threshold suggests that H^+ ions alter the activation properties of the permeation pathway. Consistent with this notion, the time required for activation of the current was found to vary markedly with pH_i (Fig. 9 *D*). In all cases, the kinetics of activation was voltage dependent, with faster opening at more positive potentials. For any given potential, however, the time required for half-maximal activation became considerably greater as the pH_i was elevated (Fig. 9 *D*). This correlation is illustrated in the inset to Fig. 9 *D*. In the range studied, there is a near linear relationship between pH_i and the activation half-time, measured at +60 mV. These data likely underestimate the regulatory effect of pH_i on the activation kinetics, because at higher pH_i values equilibration of the current was incomplete during application of the pulse. As discussed earlier, longer pulses were avoided to minimize the pH changes that occurred despite the inclusion of 100 mM buffer. On

---

was normalized as in Fig. 9 *C*. Values > 15 mV were omitted in the pH 8.1 and 7.5 curves for clarity. (*D*) Voltage dependence of the time required for half-maximal activation of the current. Maximal current was defined as that measured at the end of the 2.5-s depolarizing pulse. Data are means ± SEM of three separate experiments. (*Inset*) pH_o-dependence of the time for half-maximal activation, plotted using the mean values in *D* determined at +60 mV.

the other hand, H^+ depletion occurring during application of large pulses may have curtailed the current prematurely, causing it to peak earlier.

Effect of extracellular pH (pH_o) on H^+ conductance. The outward current was also exquisitely sensitive to changes in the extracellular pH (pH_o). As shown in Fig. 10 *A*, larger outward currents were observed at higher pH_o. For these experiments, a solution of pH 6.0 was used in the patch pipette to maximize the conductance. Maximal currents were obtained at pH_o 8.1, the highest pH compatible with stability of the patch. As was the case for the internal pH, the effects of pH_o cannot be solely accounted for by changes in the protonmotive force. As illustrated in Fig. 10 *B*, the chord conductance is sensitive to pH_o, being larger at any voltage above the threshold in more alkaline bathing media. At pH_o 8.1 and pH_i 6.0, the conductance in bilateral CsAsp was apparent around −45 mV and saturated around +30 mV at ≈0.25 nS/pF.

The voltage dependence of the permeability is illustrated in Fig. 10 *C*. As in Fig. 9, permeability was only calculated for those conditions yielding sizable currents, for accuracy. The maximal permeability attained was greater at more alkaline pH. Unlike Fig. 9, this effect is not likely due to depletion of internal H^+, because the currents and therefore the anticipated depletion were greater at more alkaline pH_o. Depletion can however account for the unexpected permeability decrease noted at high voltages at pH_o 8.1. When the data are normalized to the maximal permeability observed at each pH, the steepness of the activation curves appears to be similar at different pH_o (*inset*, Fig. 10 *C*).

The threshold for activation of the permeability was found to vary with pH_o, becoming more negative in alkaline media. Therefore, as in the case of pH_i, the external pH affected the current not only by altering the protonmotive force, but also by directly modifying the properties of the conductance. In accordance with this notion, the extracellular pH also affected the kinetics of activation of the H^+ conductance (Fig. 10 *D*). For any given voltage, more alkaline extracellular solutions decreased the half-time for activation. As shown in the inset of Fig. 10 *D*, at a constant voltage (+60 mV) the activation time increased nearly fourfold over a 2.1 pH unit interval. Together, these results indicate that the activation of the H^+ conductive pathway is dictated by multiple factors, including the transmembrane potential as well as the intra- and extracellular pH.

Inhibition by Zn^{2+}. The inhibitory effect of Zn^{2+} on the pH recovery in acid-loaded, suspended cells (Fig. 1 *B*) was paralleled by blockage of the outward currents in adherent patch-clamped cells (Fig. 11). As shown in Fig. 11 *A*, in bilateral CsAsp solutions with pH_i 6.0 and pH_o 7.5 and at +60 mV, inhibition was clearly evident at 0.2 mM and nearly complete at 2 mM. Because of the tendency of aspartate to bind Zn^{2+}, the free concentrations of the divalent cation are likely to be considerably lower than the total values listed above. The effects of Zn^{2+} on the current were entirely and readily reversible. Analysis of the current-voltage relationship revealed that the divalent cation induced a positive shift in the current activation threshold (Fig. 11 *B*). Once the threshold was reached, however, the slope of the current vs voltage relationship was similar in the presence and absence of Zn^{2+}, within the limited range of voltages compatible with stable whole-cell recordings. These findings are consistent with the notion that the primary effect of the inhibitor

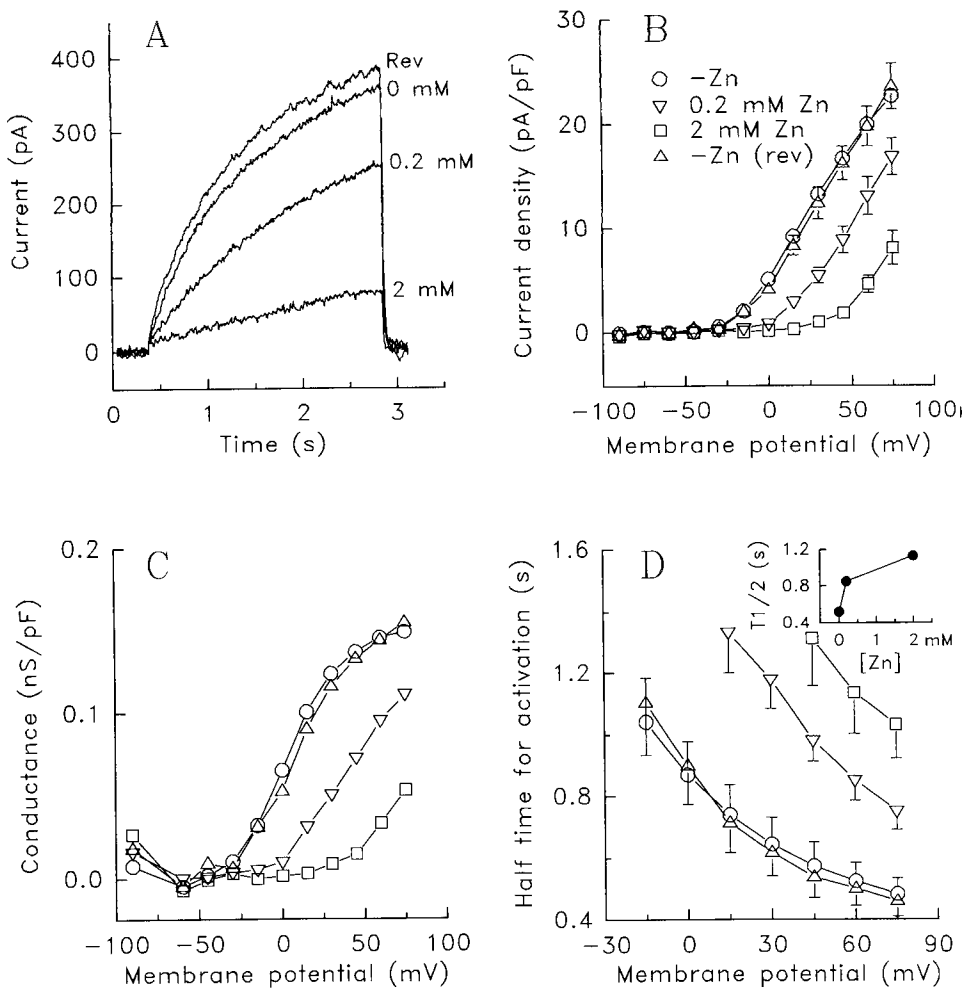

FIGURE 11. Inhibition by Zn^{2+}. Adherent macrophages were patched in the whole-cell configuration with pipettes containing solution CsAsp 6.0. The holding voltage was −60 mV. The bath was perfused successively with the following solutions: CsAsp 7.5 (*circles; −Zn*), CsAsp 7.5 + 0.2 mM Zn (*inverted triangles*), CsAsp 7.5 + 2 mM Zn (*squares*), CsAsp 7.5 (*triangles; −Zn rev*). EGTA was omitted from the solutions containing Zn^{2+}. (*A*) Representative current traces generated by depolarization to +60 mV. The concentration of Zn^{2+} used in the bath is indicated. *Rev* refers to restoration of the control (no Zn^{2+}) condition after perfusion with 2 mM Zn^{2+}. (*B*) Current-voltage relationships, generated using the protocol described in Fig. 5. Currents were normalized per capacitance. The data are means ± SEM of three experiments. Where absent, error bars were smaller than the symbol. (*C*) Conductance-voltage relationship determined using the mean values from *B* and the calculated E_{rev}, as described in Fig. 9. (*D*) Voltage dependence of the time required for half-maximal activation of the current. Maximal current was defined as that measured at the end of the 2.5-s depolarizing pulse. Data are means ± SEM of three separate experiments. (*Inset*) Zn^{2+} concentration dependence of the time for half-maximal activation, plotted using the mean values in *D* determined at +60 mV. [Zn] refers to the total Zn^{2+} concentration, which is likely to be significantly higher than the free concentration, because of interaction with aspartate and/or HEPES.

was to alter the surface potential in the vicinity of the conducting entity. This is also apparent from the conductance-voltage relationship of Fig. 11 *C*.

In addition to affecting the magnitude of the steady state current at any given potential, Zn^{2+} also modified the kinetics of activation of the conductance. The divalent cation reversibly prolonged the half-time for activation at all voltages studied (Fig. 11 *D*). Under the conditions chosen for analysis (pH_i 6.0, pH_o 7.5, and +60 mV), the presence of 2 mM Zn^{2+} lengthened the activation process nearly threefold (see inset to Fig. 11 *D*).

DISCUSSION

pH_i Recovery in Acid-Loaded Macrophages: Evidence for a Conductive Component

When macrophages are suspended in Na^+-free solutions containing bafilomycin, the Na^+/H^+ antiporters and the vacuolar-type H^+ pumps are inoperative. Nevertheless, a sizable pH_i recovery was recorded under these conditions following acid-loading (Fig. 1). Several lines of evidence indicate that this H^+ (equivalent) translocation occurs via a conductive pathway. First, the rate of pH_i recovery was considerable under conditions expected to depolarize the cells (K^+-rich medium plus valinomycin), but negligible when the cells were hyperpolarized (NMG^+-rich medium with valinomycin). Second, the rate of H^+ translocation was accelerated by valinomycin, ostensibly by providing a conductive pathway for counterion permeation. Third, intracellular alkalinization was readily induced in patch-clamped cells by setting the voltage to depolarizing potentials (Fig. 2). In these experiments, the rate and extent of the pH_i changes correlated with the magnitude of the outward H^+ current observed to appear concomitantly during the pulse. Together, these observations suggest that H^+ extrusion from acid-loaded macrophages can occur in part through a conductive pathway.

Evidence that the Outward Current Is Carried Primarily by H^+

A comparatively large outward current was recorded in macrophages at depolarizing potentials (e.g. Figs. 2, 3, and 5). Several independent criteria indicate that H^+ (equivalents) constitute the primary transported species. Substitution experiments demonstrated that the magnitude and direction of the current was virtually unaffected by replacement of the major ionic species with large, purportedly impermeant organic or inorganic ions. Moreover, the E_{rev} derived from analysis of the tail currents differed markedly from the equilibrium potentials of the major ions and was insensitive to large changes in their concentration (Fig. 7 and Table II). Instead, E_{rev} varied drastically when the transmembrane ΔpH was altered and generally approached, but was not equal to the calculated E_{H^+} (Fig. 7). The observed deviations of the measured E_{rev} from the predicted E_{H^+} could be attributed to one or more of the following reasons: (*a*) it is conceivable that ions other than H^+ (equivalent) can permeate the depolarization-induced pathway. Given the relative concentrations of H^+ and of the main ionic constituents of the media, the permeability of the pathway to the latter need not be large to account for the observed discrepancy between E_{rev} and E_{H^+} (see below); (*b*) the cytosolic pH, particularly that of the submembranous space, may not be identical to that of the pipette filling solution. This is likely to be

the case, especially after application of the conditioning pulse that preceded measurement of the tail current. Even when using heavily buffered solutions, the large amount of acid equivalents mobilized by the current is expected to result in significant cytosolic pH changes (see Fig. 8 and discussion below).

Further evidence that H^+ (equivalents) are largely responsible for the outward current is provided by the similar potential dependence of the voltage-induced pH_i changes and of the accompanying current. As summarized in Fig. 4, when the starting pH_i is 6.5, neither current nor net H^+ translocation are detectable below −30 mV. At more positive potentials, outward current and H^+ (equivalent) efflux develop in parallel, strongly suggesting an intimate relationship between these events. Moreover, both the current and the cytosolic alkalinization are inhibited by Zn^{2+}.

The minimum number of H^+ equivalents required to account for the observed changes in pH_i can be estimated, if reasonable assumptions are made regarding the internal buffering power of patched cells (see Results). For a cell with a typical volume of 700 fl (determined by electronic sizing with the Coulter-Channelyzer), a ΔpH of 0.8 U such as that elicited by a 7-s pulse in Fig. 3 *A*, would require mobilization of 2.2×10^{-15} to 1.7×10^{-14} mol ($2.2–17 \times 10^{-10}$ C) of charged H^+ equivalents. Assuming that the cells are spherical and that their plasma membrane has a capacitance of 1 $\mu F/cm^2$, the current associated with the movement of H^+ equivalents would therefore range between 2 and 16 pA/pF. Clearly, this is a minimum estimate, to the extent that buffer molecules can diffuse from the pipette into the cell during the period of current injection. Even with these limitations, the calculated value is of the same order as the measured current (≈10 pA/pF). Together with the ionic specificity and E_{rev} determinations, the temporal and quantitative correlation between the current and pH_i changes indicates that H^+ (equivalents) mediate the outward current. Because at constant external pH the maximal conductance increased as pH_i was lowered, it could be argued that H^+, rather than OH^-, HCO_3^- or other acid equivalents, are the charge carrier. However, this criterion is not definitive because, as discussed below, internal acidification also exerts allosteric effects on the conductive pathway.

Perusal of the ionic substitution data summarized in Table II suggests that the conductance is extremely selective for H^+. While accurate estimates of the ionic selectivity cannot be provided at present, the relative permeabilities can be roughly estimated using the Goldman-Hodgkin-Katz equation. Thus, the largest deviation of the measured E_{rev} from the calculated E_{H^+} (i.e., ≈45 mV when ΔpH = 2.1; see Fig. 7) could be accounted for assuming that the major monovalent cation is ~1,000,000-fold less permeant than H^+. The estimated selectivity is even greater when experiments using smaller pH gradients are used for the calculation, because E_{rev} more closely approximates E_{H^+} under these conditions (Fig. 7).

Properties of the H^+ Current

Several properties of the current are noteworthy and likely of biological significance. First, the conductance is markedly voltage-dependent, increasing at more positive potentials. Thus, steady state current vs voltage relationships display sharp outward rectification. This apparent rectification is a property of the activation process and does not reflect the behavior of the open conductive pathway. Tail current analysis

demonstrated the latter to be approximately symmetrical, because the instantaneous current-voltage relationship was nearly linear. The slight deviation from linearity could be explained by asymmetric substrate distribution and/or rapid, voltage-dependent deactivation (see Results).

When compared to other voltage-sensitive currents of macrophages, the activation kinetics of the H^+ current are remarkably slow (Gallin and McKinney, 1988; Nelson, Jow, and Jow, 1990; Gallin, 1991). At negative membrane potentials, the kinetics were often sigmoidal and in excess of 1 s was required for half-maximal activation of the conductance (e.g., Fig. 9). The rate of activation was greater at more positive potentials (Figs. 9 and 10) and the sigmoidicity became less apparent. On the other hand, deactivation upon repolarization was more rapid and could be fitted by a single exponential (not shown).

The rate and extent of activation of the conductance were also a function of the intracellular pH. More acidic solutions favored the outward current, an effect that was not entirely attributable to increased protonmotive force or substrate availability. Calculations of the permeability, which correct for the changing driving force and substrate concentration as pH_i is varied, indicated that the activation process is directly modulated by the intracellular H^+ concentration. Consistent with this possibility is the observation that the time required for activation of the conductance at any given potential was noticeably shortened at lower pH_i. The primary effect of lowering pH_i was to displace the activation threshold to more negative voltages. These findings are consistent with titration of ionizable groups that alter the fixed charge near the conductive pathway, reducing the surface potential.

The extracellular pH also affected the conductance. The voltage dependence of the permeability was shifted to more positive potentials as the medium was acidified. In addition, the maximal permeability was somewhat decreased at low pH_o. As before, changes in surface potential by charge neutralization can account for the effects of pH_o on the activation threshold. However, a different process may be involved in reducing the maximal permeability. Zn^{2+} too alters the voltage dependence of the activation kinetics, and its effects can similarly be explained by assuming that the divalent cation reduces the negativity of the extracellular surface potential. Because all media contained 1 mM Mg^{2+} and high concentrations of monovalent cations, a double-layer screening effect of Zn^{2+} is unlikely and specific binding to a site on or near the conductive entity is suggested.

In the absence of blockers, a gradual decrease of the current was observed during prolonged depolarization (Fig. 8). However, this apparent inactivation did not reflect an intrinsic property of the conductance but rather was a consequence of the changing ionic environment in the vicinity of the membrane. Despite the large buffering capacity of the patch pipette, significant pH_i changes were induced by the passage of current, as evidenced by direct measurements using BCECF and by the shift in the E_{rev}. The occurrence of cytosolic pH changes in small cells patched in the whole-cell configuration might appear surprising. However, diffusion of H^+ and/or buffers from the pipette into the cell was found to be slow compared to the transmembrane flow of H^+ equivalents through the conductance. This can be appreciated in Fig. 3, where recovery of the initial pH after termination of the pulse required 2–3 min even when heavily buffered pipette-filling solutions were used.

After long pulses, the pH of the unstirred layer of external medium surrounding the cell is also likely to have changed significantly. This could be inferred from the measured reversal potential and intracellular pH. After 9 s, E_{rev} was −15 mV and pH_i increased to 6.95, implying that pH_o in the vicinity of the cell dropped from 7.5 to 7.3. These calculations assume that the average intracellular pH measured photometrically adequately reflects H^+ activity at the cytosolic face of the membrane. Changes in the surface pH of snail neurons during application of depolarizing pulses were earlier reported by Thomas (1988). In summary, the decrease of the current was attributable to intracellular and possibly also extracellular pH changes, but no evidence was obtained for voltage or time-dependent inactivation of the conductance, a feature that may be important for sustained H^+ extrusion during prolonged macrophage activation.

Comparison with Other Currents

A slowly activating current was described earlier in human macrophages, which shares several features with the H^+ current described here. Nelson et al. (1990) detected an outward rectifying current that was inhibited by Zn^{2+}. The current was designated as a "nonselective" cation current based on the observation that the conductance was similar in Cs^+, K^+, and Na^+ solutions. These findings, however, are equally compatible with a H^+ conductance. It is therefore conceivable that the current reported here had been earlier detected in monocyte-derived human macrophages by Nelson et al. (1990).

As mentioned in the Introduction, H^+ selective currents were initially described in snail neurons (Thomas and Meech, 1982; Byerly et al., 1984; Byerly and Suen, 1989). Comparable currents were later found in oocytes of the axolotl *Ambystoma* (Barish and Baud, 1984) and recently in alveolar epithelial cells (DeCoursey, 1991) and in granulocytic HL60 cells (Demaurex et al., 1993). The currents in these cell types share many similarities, including outward rectification, sensitivity to internal and external pH and inhibition by heavy metals (Thomas and Meech, 1982; Byerly et al., 1984; Byerly and Suen, 1989; Mahaut-Smith, 1989; DeCoursey, 1991; Demaurex et al., 1993). All of these currents activate comparatively slowly, but large differences in kinetics exist between cell types. Snail neurons activate within 25 ms (Thomas and Meech, 1982; Byerly et al., 1984; Byerly and Suen, 1989), whereas up to 300 ms are required in the case of oocytes (Barish and Baud, 1984). As was found for macrophages, even longer times (>1 s) are sometimes necessary for current activation in epithelial cells (DeCoursey, 1991) and in HL60 cells (Demaurex et al., 1993). These differences in activation kinetics may reflect the specific physiological role of the conductance in individual tissues. Rapid opening of channels may be required in neurons, which depolarize for short periods, while a more slowly reactive conductance is compatible with the sustained depolarization reported in activated phagocytes (Gallin, 1991).

Proton currents may also exist in other cells. A "residual" outward current has been described in a couple of cell types subjected to ion substitution or to inhibitors of established channels (Kostyuk and Krishtal, 1977; Byerly and Hagiwara, 1982). The properties of these residual currents are consistent with an outward H^+ conductance. On the other hand, H^+ currents of the magnitude described here are unlikely to be

ubiquitous. The success reported in measuring the reversal potential of Ca^{2+} currents, at near physiological Ca^{2+} concentrations (e.g., Lee and Tsien, 1982; Fukushima and Hagiwara, 1985), argues against the presence of sizable H^+ currents. The large positive potentials needed to approach the Ca^{2+} equilibrium potential would be expected to unmask the H^+ conductance, which was not detected in these studies. It is conceivable, nevertheless, that the internal pH of these cells was high and that the threshold for H^+ current activation was never attained.

Under optimal conditions, the limiting H^+ conductance of macrophages reached 0.25 nS/pF. This value is one to four times larger than the specific conductance that can be estimated from data published for neurons, oocytes and alveolar cells (Byerly and Suen, 1989; Barish and Baud, 1984; DeCoursey, 1991). It is also interesting to note that the H^+ conductance is of the same order as other inorganic ion conductances of mammalian macrophages (Gallin and McKinney, 1988; Nelson et al., 1990; Gallin, 1991). Moreover, contrary to the effects reported here for the H^+ conductance, the K^+ conductance of many mammalian cells decreases as pH_i is lowered. In view of the relative magnitude of the H^+ and K^+ conductances, it becomes clear why an exogenous ionophore (valinomycin) was required in Fig. 1 to provide the counterion permeability necessary to express maximal rates of net H^+ translocation.

Possible Physiological Role of the H^+ Current

The data summarized above define a H^+ specific pathway of high transport capacity. The enormous selectivity of the system for H^+ over other ions is suggestive of a role in pH regulation. In macrophages, maintenance of pH_i is challenged during stimulation of the cells in the course of infection or inflammation. In this instance, the metabolic rate of the cells is greatly elevated, in part by activation of the NADPH oxidase and the hexose monophosphate shunt (Rossi, 1986; Clark, 1990). The by-products of these reactions include H^+ (and equivalents), which tend to acidify the cytosol (Swallow et al., 1988). In principle, activation of a H^+ conductive pathway can help counteract this tendency. Several features of the H^+ current described here make it suitable for this role. First, the conductance is activated by internal acidification, favoring faster extrusion when metabolism is activated and pH_i begins to drop. Secondly, external alkalinization activates the conductance. The extracellular dismutation of superoxide produced by the NADPH is predicted to elevate the local pH, further facilitating H^+ efflux. Conversely, acidification of the phagosomal space (which is topologically outside) will inhibit the conductive pathway. This feature would prevent dissipation of the phagosomal acidification generated by the vacuolar H^+ pumps (Lukacs et al., 1990). Finally, the conductance appears to be exquisitely voltage dependent. At the E_m known to prevail in unstimulated cells (−50 to −60 mV; see Gallin, 1991 and Nanda and Grinstein, 1991*b*, for reviews), the permeability through this pathway would be negligible, precluding electrophoretic acid loading of resting cells. In contrast, the conductance would become active when the cells are stimulated. Activation of phagocytes, including macrophages, by a variety of stimuli is known to produce a large, sustained depolarization (Gallin, 1991; Nanda and Grinstein, 1991*b*). Together with the incipient acidification and external alkalinization, the change in E_m would be conducive to activation of the H^+ permeability. Though the precise magnitude of the depolarization remains debatable (see Gallin,

1991 and Nanda and Grinstein, 1991*b*, for reviews), the combined electrochemical H^+ gradient under these conditions is most likely to point outward. Therefore, a conductive flux would be in the direction of net H^+ extrusion, favoring pH_i regulation.

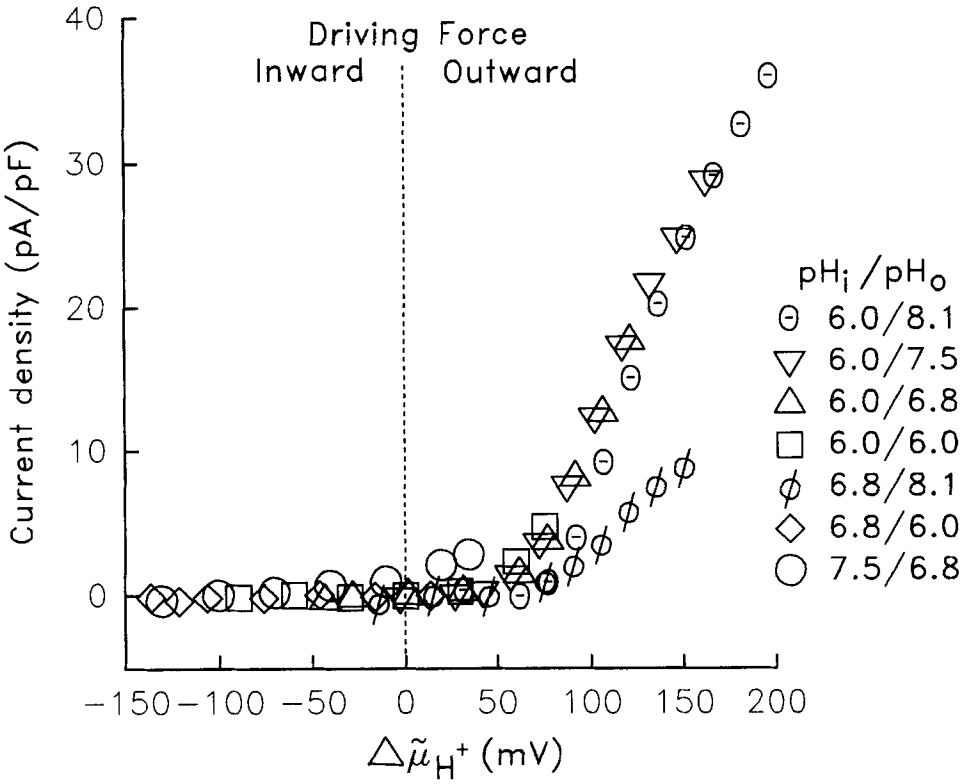

FIGURE 12. Force vs flow relationship of the H^+ current. The graph shows the current (ordinate) as a function of its driving force, i.e., the electrochemical H^+ gradient (abscissa). Current was measured as described in Fig. 5 under a variety of experimental conditions. The major salt in all cases was CsAsp and the intra- and extracellular pH combinations used are identified on the figure. The driving force ($\Delta\mu_{H^+}$) was calculated as

$$\Delta\mu_{H^+} = E_m - 58(pH_i - pH_o),$$

where E_m is the applied membrane potential and pH_i and pH_o are the internal and external pH, respectively. Positive values indicate net outward force and viceversa. Current densities were calculated by normalizing per cell capacitance. Points are means of three experiments. Error bars were omitted for graphic clarity.

The mechanism responsible for the depolarization of phagocytes has not been entirely clarified. As proposed initially by Henderson et al. (1987), the potential change could result from the operation of the purportedly electrogenic NADPH oxidase. This membrane-bound enzymatic complex releases superoxide anions to the

medium while $NADP^+$ and H^+ are liberated into the cytosolic compartment. If the oxidase were in fact electrogenic, parallel translocation of a counterion would be required to support sustained secretion of reactive oxygen metabolites. Protons extruded by the conductive pathway could also serve such a role. In this manner, the oxidase would not only contribute to the generation of metabolic acid, but would also provide the driving force needed for some of its removal. The currents detected here could readily provide sufficient current to neutralize the charge displaced by the oxidase. The reported rates of superoxide production by macrophages approach 1 nmol/10^6 cells min (Johnston, Godzik, and Cohn, 1978; Johnson and Sung, 1987). Assuming that two net charges are displaced per superoxide synthesized, the oxidase would generate a current equivalent to 3.2 pA/cell. Because the average capacitance of the cells was 16 pF, this corresponds to a current density of 0.2 pA/pF, which is considerably smaller than the maximal H^+ currents detected ($\approx$ 10–30 pA/pF). It is relevant that electroneutral pH regulating systems such as the Na^+/H^+ and Cl^-/HCO_3^- exchangers, while capable of effective H^+ equivalent translocation, would be unable to compensate the rheogenic effect of the NADPH oxidase or to utilize the driving force that it generates.

Fig. 12 illustrates a remarkable property of the H^+ conductive pathway. The graph is a force ($\Delta\tilde{\mu}_{H^+}$) vs flow plot summarizing data obtained under a large number of conditions, including various combinations of pH_i and pH_o and a wide range of membrane potentials (from −90 to +75 mV). Regardless of the experimental conditions, only outward fluxes of H^+ were ever detectable. It therefore appears that the conductance activation process ensures that net acid uptake will never occur. This may be of crucial importance when activated macrophages penetrate the acidic environment of abscesses or tumors.

A conductive H^+ permeability was described in neutrophils stimulated with phorbol esters (Nanda and Grinstein, 1991*a;* Kapus et al., 1992) or with arachidonate (Henderson and Chappell, 1992). A similar permeability has also been detected in suspensions of murine macrophages using macroscopic pH_i determinations (A. Yi Qu, unpublished observations). The relationship of the latter permeability with the H^+ current described here is not clear. Both are sensitive to Zn^{2+}, suggesting that the same molecular entity is involved in both processes. It is conceivable that arachidonate or stimuli of protein kinase C activate the H^+ conductance by modifying its sensitivity to pH_i, pH_o or to the membrane potential. These possibilities are currently under investigation.

We are grateful to Drs. M. Salter, J. MacDonald, and P. Pennefather for their advice and support during the course of these studies. We also thank Drs. G. Brisseau and X. Zhao for providing macrophages.

Supported by the Medical Research Council (MRC) of Canada and the Canadian Cystic Fibrosis Foundation. A. Kapus is the recipient of a MRC postdoctoral fellowship. The Soros Foundation provided financial support to cover the travel expenses of A. Kapus. S. Grinstein is cross-appointed to the Department of Biochemistry of the University of Toronto and is an International Scholar of the Howard Hughes Medical Institute.

Original version received 19 November 1992 and accepted version received 20 May 1993.

REFERENCES

Barish, M. E., and C. Baud. 1984. A voltage-gated hydrogen ion current in the oocyte membrane of the axolotl, *Ambystoma*. *Journal of Physiology*. 352:243–263.

Barry, P. H., and J. W. Lynch. 1991. Liquid junction potentials and small cell effects in patch-clamp analysis. *Journal of Membrane Biology*. 121:101–117.

Bidani, A., S. E. S. Brown, T. A. Heming, R. Gurich, and T. D. DuBose. 1989. Cytoplasmic pH in pulmonary macrophages: recovery from an acid load is Na^+ independent and NEM sensitive. *American Journal of Physiology*. 257:C56–C76.

Bowman, E. J., A. Siebers, and K. Altendorf. 1988. Bafilomycins: A class of inhibitors of membrane ATPases from microorganisms, animal cells and plant cell. *Proceedings of the National Academy of Sciences, USA*. 85:7972–7976.

Byerly, L., and S. Hagiwara. 1982. Calcium currents in internally perfused nerve cell bodies of *Limnea digitalis*. *Journal of Physiology*. 322:503–528.

Byerly, L., R. Meech, and W. Moody. 1984. Rapidly activating hydrogen ion currents in perfused neurons of the snail, *Lymnaea stagnalis*. *Journal of Physiology*. 351:199–216.

Byerly, L., and Y. Suen. 1989. Characterization of proton currents in neurons of the snail *Lymnaea stagnalis*. *Journal of Physiology*. 413:75–89.

Clark, R. A. 1990. The human neutrophil respiratory burst oxidase. *Journal of Infectious Diseases*. 161:1140–1147.

DeCoursey, T. E. 1991. Hydrogen ion currents in rat alveolar epithelial cells. *Biophysical Journal*. 60:1243–1253.

Demaurex, N., S. Grinstein, M. Jaconi, W. Schlegel, D. P. Lew, and K. H. Krause. 1993. Proton currents in HL60 granulocytes: regulation by membrane potential and intracellular pH. *Journal of Physiology*. 466:329–344.

Fukushima, Y., and S. Hagiwara. 1985. Currents carried by monovalent cations through calcium channels in mouse neoplastic B lymphocytes. *Journal of Physiology*. 358:255–284.

Gallin, E. K. 1991. Ion channels in leukocytes. *Physiological Reviews*. 71:775–811.

Gallin, E., and L. C. McKinney. 1988. Patch-clamp studies of human macrophages: Single channel and whole-cell characterization of two K^+ conductances. *Journal of Membrane Biology*. 103:55–66.

Grinstein, S., and W. Furuya. 1986. Cytoplasmic pH regulation in phorbol ester-activated human neutrophils. *American Journal of Physiology*. 251:C55–C65.

Hamill, O. P., A. Marty, E. Neher, B. Sakman, and F. Sigworth. 1981. Improved patch-clamp techniques for high resolution current recording from cells and cell-free membrane patches. *Pflügers Archiv*. 391:85–100.

Henderson, L. M., and J. B. Chappell. 1992. The NADPH-oxidase-associated H^+ channel is opened by arachidonate. *Biochemical Journal*. 283:171–177.

Henderson, L. M., J. B. Chappell, and O. T. G. Jones. 1987. The superoxide-generating NADPH oxidase of human neutrophils is electrogenic and associated with an H channel. *Biochemical Journal*. 246:325–329.

Henderson, L. M., J. B. Chappell, and O. T. G. Jones. 1988. Internal pH changes associated with the activity of the NADPH oxidase: further evidence for the presence of a H^+ conducting channel. *Biochemical Journal*. 251:563–567.

Hille, B. 1992. Ionic channels of excitable membranes. Sinauer Associates Inc., Sunderland, MA. 607 pp.

Johnson, W. J., and C. Sung. 1987. RAt macrophage treatment with lipopolysaccharide leads to a reduction in respiratory burst product secretion. *Cellular Immunology*. 108:109–119.

Johnston, R. B., C. A. Godzik, and Z. A. Cohn. 1978. Increased superoxide anion production by immunologically activated and chemically elicited macrophages. *Journal of Experimental Medicine.* 148:115–127.

Kapus, A., K. Szaszi, and E. Ligeti. 1992. Phorbol 12-myristate 13-acetate activates an electrogenic H^+ conducting pathway in the membrane of neutrophils. *Biochemical Journal.* 281:697–701.

Kostyuk, P. G., and O. A. Krishtal. 1977. Separation of sodium and calcium currents in the somatic membrane of mollusc neurones. *Journal of Physiology.* 270:545–568.

Lee, K. S., and R. W. Tsien. 1982. Reversal of current through calcium channels in dialyzed single heart cells. *Nature.* 297:498–501.

Lukacs, G. L., O. D. Rotstein, and S. Grinstein. 1990. Phagosomal acidification is mediated by a vacuolar-type H^+ ATPase in murine macrophages. *Journal of Biological Chemistry.* 265:21099–21107.

Mahaut-Smith, M. P. 1989. The effect of zinc on calcium and hydrogen ion currents in intact snail neurons. *Journal of Experimental Biology.* 145:455–464.

Molski, T. F. P., P. H. Naccache, M. Volpi, L. M. Wolpert, and R. I. Sha'afi. 1980. Specific modulation of the intracellular pH of rabbit neutrophils by chemotactic factors. *Biochemical and Biophysical Research Communications.* 94:508–514.

Nanda, A., and S. Grinstein. 1991*a*. Protein kinase C activates an H^+ (equivalent) conductance in the plasma membrane of human neutrophils. *Proceedings of the National Academy of Sciences, USA.* 88:10816–10820.

Nanda, A., and S. Grinstein. 1991*b*. The membrane potential of resting and activated neutrophils: determinants and significance. *Cellular Physiology and Biochemistry.* 1:65–75.

Nelson, D. J., B. Jow, and F. Jow. 1990. Whole-cell currents in macrophages: I. Human monocyte-derived macrophages. *Journal of Membrane Biology.* 117:29–44.

Roos, A., and W. F. Boron. 1981. Intracellular pH. *Physiological Reviews.* 61:296–434.

Rossi, F. 1986. The superoxide-forming NADPH oxidase of the phagocytes: Nature, mechanisms of activation and function. *Biochimica et Biophysica Acta.* 853:65–89.

Sha'afi, R. I., and T. F. Molski. 1988. Activation of the neutrophil. *Progress in Allergy.* 42:1–64.

Simchowitz, L., and E. J. Cragoe. 1987. Intracellular acidification-induced alkali metal cation/H^+ exchange in huma neutrophil. *Journal of General Physiology.* 90:737–762.

Swallow, C. J., S. Grinstein, and O. D. Rotstein. 1988. Cytoplasmic pH regulation in macrophages by an ATP-dependent and dicyclohexylcarbodiimide-sensitive mechanism. Possible involvement of a plasma membrane proton pump. *Journal of Biological Chemistry.* 263:19558–19563.

Swallow, C. J., S. Grinstein, and O. D. Rotstein. 1990. Regulation of cytoplasmic pH in resident and activated peritoneal macrophages. *Biochimica et Biophysica Acta.* 1022:203–210.

Thomas, J. A., R. N. Buchsbaum, A. Zimniak, and E. Racker. 1979. Intracellular pH measurements in Ehrlich ascites tumour cells utilizing spectroscopic probes generated *in situ*. *Biochemistry.* 18:2210–2218.

Thomas, R. C. 1988. Changes in the surface pH of voltage-clamped snail neurones apparently caused by H^+ fluxes through a channel. *Journal of Physiology.* 398:313–327.

Thomas, R. C., and R. W. Meech. 1982. Hydrogen ion currents and intracellular pH in depolarized voltage-clamped snail neurones. *Nature.* 299:826–828.